Granular Avalanches

Nico Gray, School of Mathematics, The University of Manchester

Mount St Helens May 18, 1980

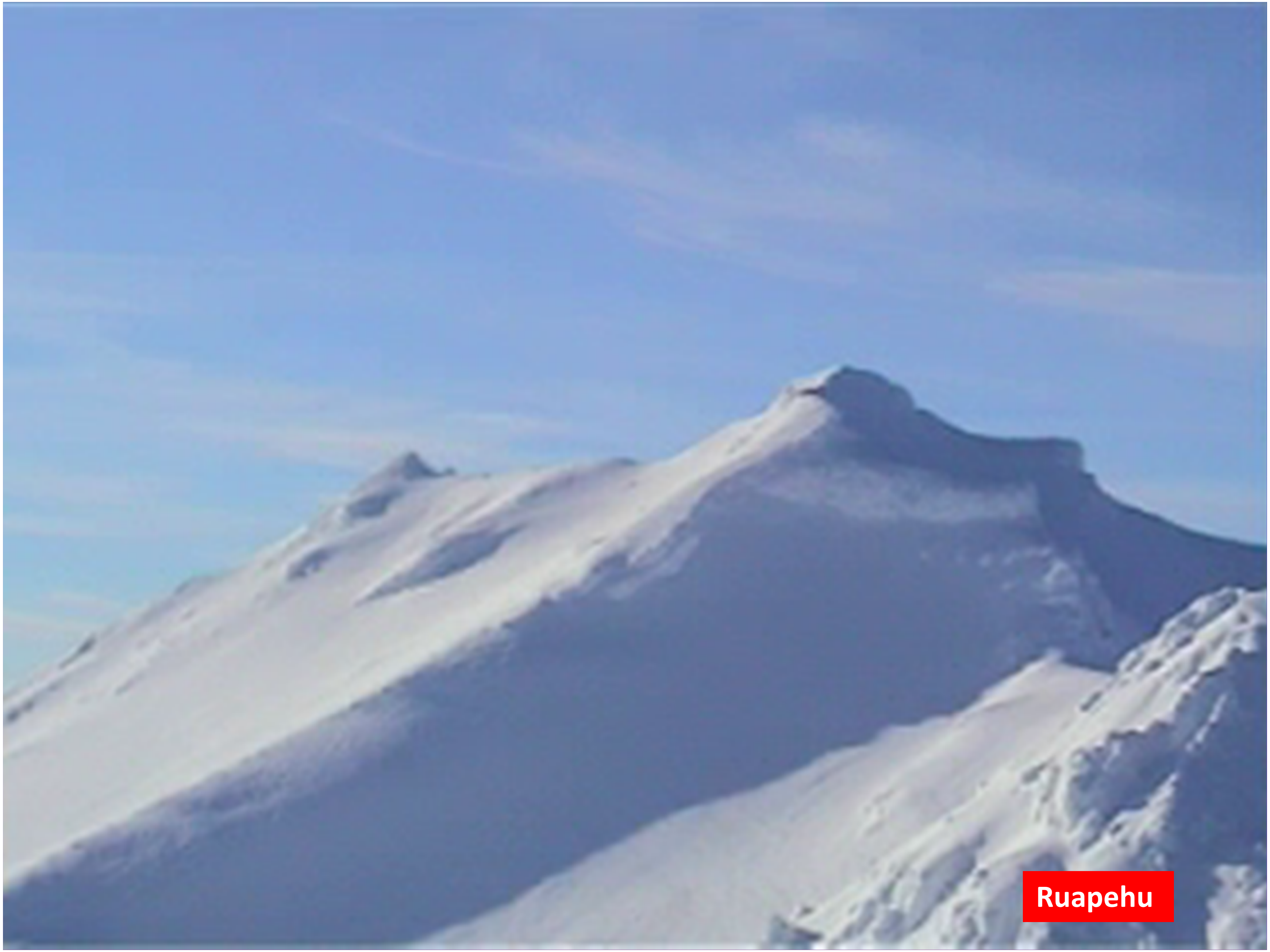
Ruapehu

Experimental chute setup and coordinate system

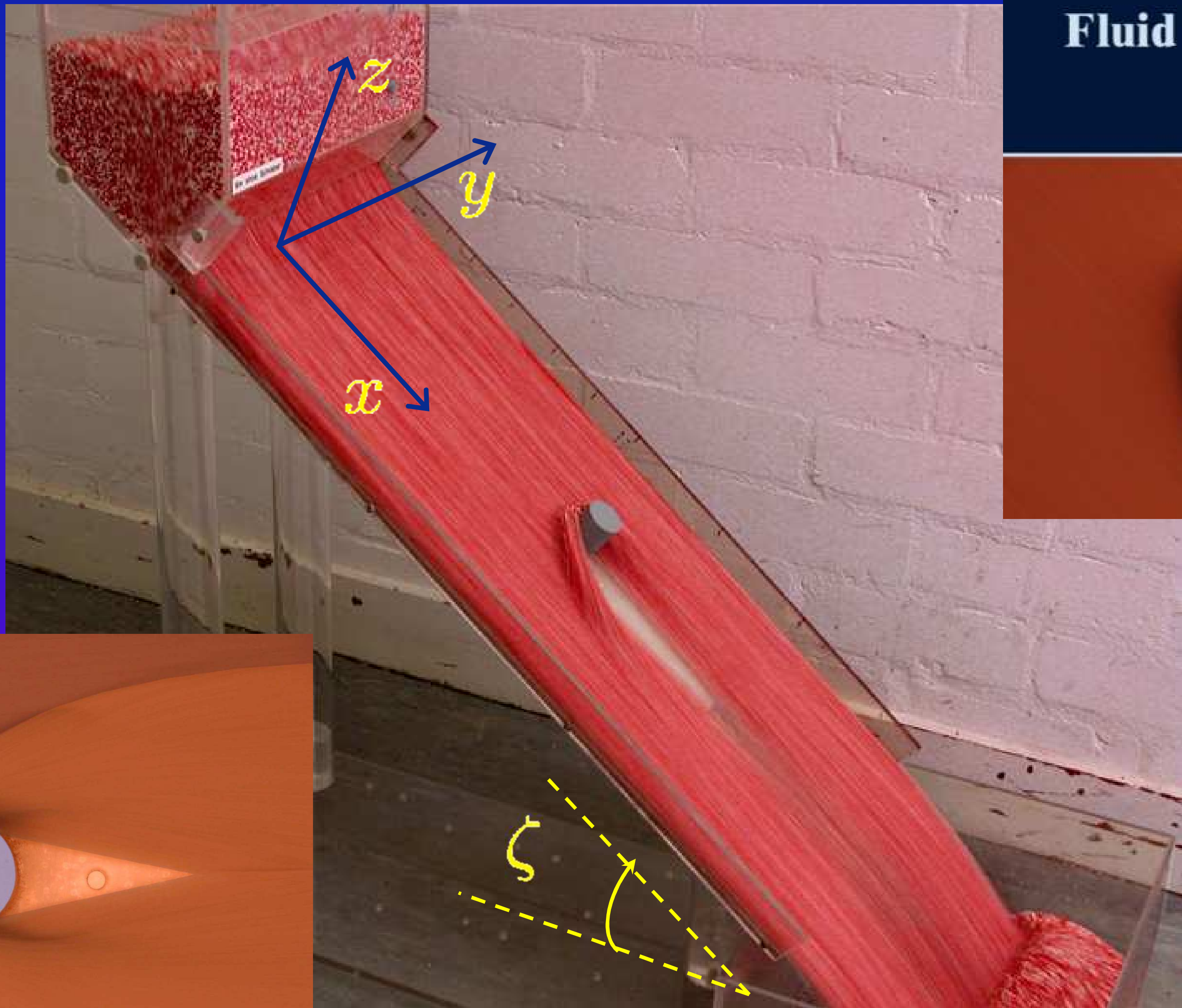

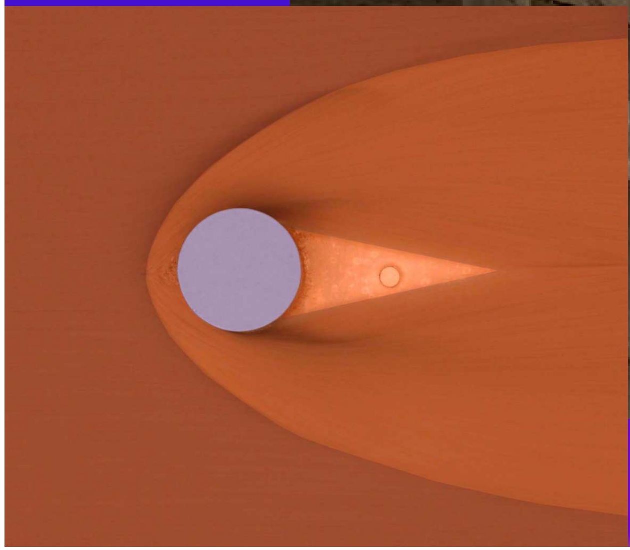

Cui & Gray *J. Fluid. Mech.*, **720**, 314-337.

Derivation of the depth-averaged equations

- Mass and momentum balances

$$\nabla \cdot \boldsymbol{u} = 0$$
$$\frac{\partial}{\partial t}(\rho \boldsymbol{u}) + \nabla \cdot (\rho \boldsymbol{u} \otimes \boldsymbol{u}) = \nabla \cdot \boldsymbol{\sigma} + \rho \boldsymbol{g},$$

- assume density ρ constant
- bulk velocity $\boldsymbol{u} = (u, w)^T$ and $\otimes$ is the dyadic product
- stress $\boldsymbol{\sigma}$ split into a pressure p and a deviatoric part $\boldsymbol{\tau}$

$$\sigma = -p\mathbf{1} + \boldsymbol{\tau}$$

- subject to kinematic conditions at surface and base

$$\frac{\partial z}{\partial t} + u\frac{\partial z}{\partial x} - w = 0, \quad \text{at} \quad z = s(x,t) \quad \text{and} \quad z = b(x,t),$$

- and surface and basal traction conditions

$$\begin{aligned} z = s(x,t): & \qquad \boldsymbol{\sigma n} = \mathbf{0}, \\ z = b(x,t): & \qquad \boldsymbol{\sigma n} = -(\boldsymbol{u}/|\boldsymbol{u}|)\mu(\boldsymbol{n}\cdot\boldsymbol{\sigma n}) + \boldsymbol{n}(\boldsymbol{n}\cdot\boldsymbol{\sigma n}), \end{aligned}$$

where $\boldsymbol{n}$ is the normal and μ is the friction coefficient.

- integrate $\nabla \cdot \boldsymbol{u} = 0$ through depth using Leibniz' Rule

$$\frac{\partial}{\partial \lambda} \int_{b(\lambda)}^{s(\lambda)} f \, dz = \int_{b(\lambda)}^{s(\lambda)} \frac{\partial f}{\partial \lambda} \, dz + \left[f \frac{\partial z}{\partial \lambda} \right]_{b(\lambda)}^{s(\lambda)},$$

- to exchange the order of integration and differentiation

$$\int_{b(x,t)}^{s(x,t)} \left(\frac{\partial u}{\partial x} + \frac{\partial w}{\partial z} \right) dz = \frac{\partial}{\partial x} \left(\int_{b(x,t)}^{s(x,t)} u \, dz \right) - \left[u \frac{\partial z}{\partial x} - w \right]_{b(x,t)}^{s(x,t)}.$$

- Defining the depth-averaged velocity and thickness

$$\bar{u} = \frac{1}{h} \int_b^s u \, dz, \qquad h(x,t) = s(x,t) - b(x,t)$$

- and using the kinematic boundary conditions the depth-averaged mass balance becomes

$$\frac{\partial h}{\partial t} + \frac{\partial}{\partial x}(h\bar{u}) = 0.$$

- Making the shallowness approximation the normal momentum balance implies pressure p is lithostatic

$$p = \rho g(s - z)\cos\zeta$$

- depth-averaging the downslope momentum balance

$$\rho\left(\frac{\partial}{\partial t}(h\overline{u}) + \frac{\partial}{\partial x}(h\overline{u^2})\right) - \left[\rho u\left(\frac{\partial z}{\partial t} + u\frac{\partial z}{\partial x} - w\right)\right]_b^s$$
$$= \rho g h\sin\zeta + \frac{\partial}{\partial x}(h\overline{\sigma_{xx}}) - \left[\sigma_{xx}\frac{\partial z}{\partial x} - \sigma_{xz}\right]_b^s.$$

- Using the kinematic and traction conditions

$$\frac{\partial}{\partial t}(h\overline{u}) + \frac{\partial}{\partial x}(\chi h\overline{u}^2) + \frac{\partial}{\partial x}\left(\frac{1}{2}gh^2\cos\zeta\right) = hgS + \frac{1}{\rho}\frac{\partial}{\partial x}(h\overline{\tau}_{xx})$$

where the shape factor and the source terms are

$$\chi = \frac{\overline{u^2}}{\overline{u}^2} \qquad S = \cos\zeta(\tan\zeta - \mu(\bar{u}/|\bar{\mathbf{u}}|)) - \frac{\partial b}{\partial x}\cos\zeta$$

- Usually the in-plane deviatoric stress $\overline{\tau}_{xx}$ is neglected and the shape factor is assumed to be unity $\chi = 1$

- Equations reduce to a hyperbolic system

$$\frac{\partial h}{\partial t} + \frac{\partial}{\partial x}(h\bar{u}) = 0$$

$$\frac{\partial}{\partial t}(h\overline{u}) + \frac{\partial}{\partial x}(h\overline{u^2}) + \frac{\partial}{\partial x}\left(\frac{1}{2}gh^2\cos\zeta\right) = hgS$$

- These can be expanded and written in matrix form as

$$\frac{\partial \boldsymbol{w}}{\partial t} + \boldsymbol{A}\frac{\partial \boldsymbol{w}}{\partial x} = \boldsymbol{g}S$$

- where

$$\boldsymbol{w} = \begin{pmatrix} h \\ \overline{u} \end{pmatrix}, \qquad \boldsymbol{A} = \begin{pmatrix} \overline{u} & h \\ g\cos\zeta & \overline{u} \end{pmatrix}, \qquad \boldsymbol{S} = \begin{pmatrix} 0 \\ S \end{pmatrix}$$

- The eigenvalues of $\boldsymbol{A}$ are given by $\det(\boldsymbol{A} - \lambda\mathbf{1}) = 0$

$$\Rightarrow (\overline{u} - \lambda)^2 - gh\cos\zeta = 0 \quad \Rightarrow \quad \lambda = \overline{u} \pm \sqrt{gh\cos\zeta}$$

- The Froude number $\mathrm{Fr} = \overline{u}/c$ is defined as the flow speed $\overline{u}$ divided by the gravity wave speed $c = \sqrt{gh\cos\zeta}$

Upslope propagating granular bores

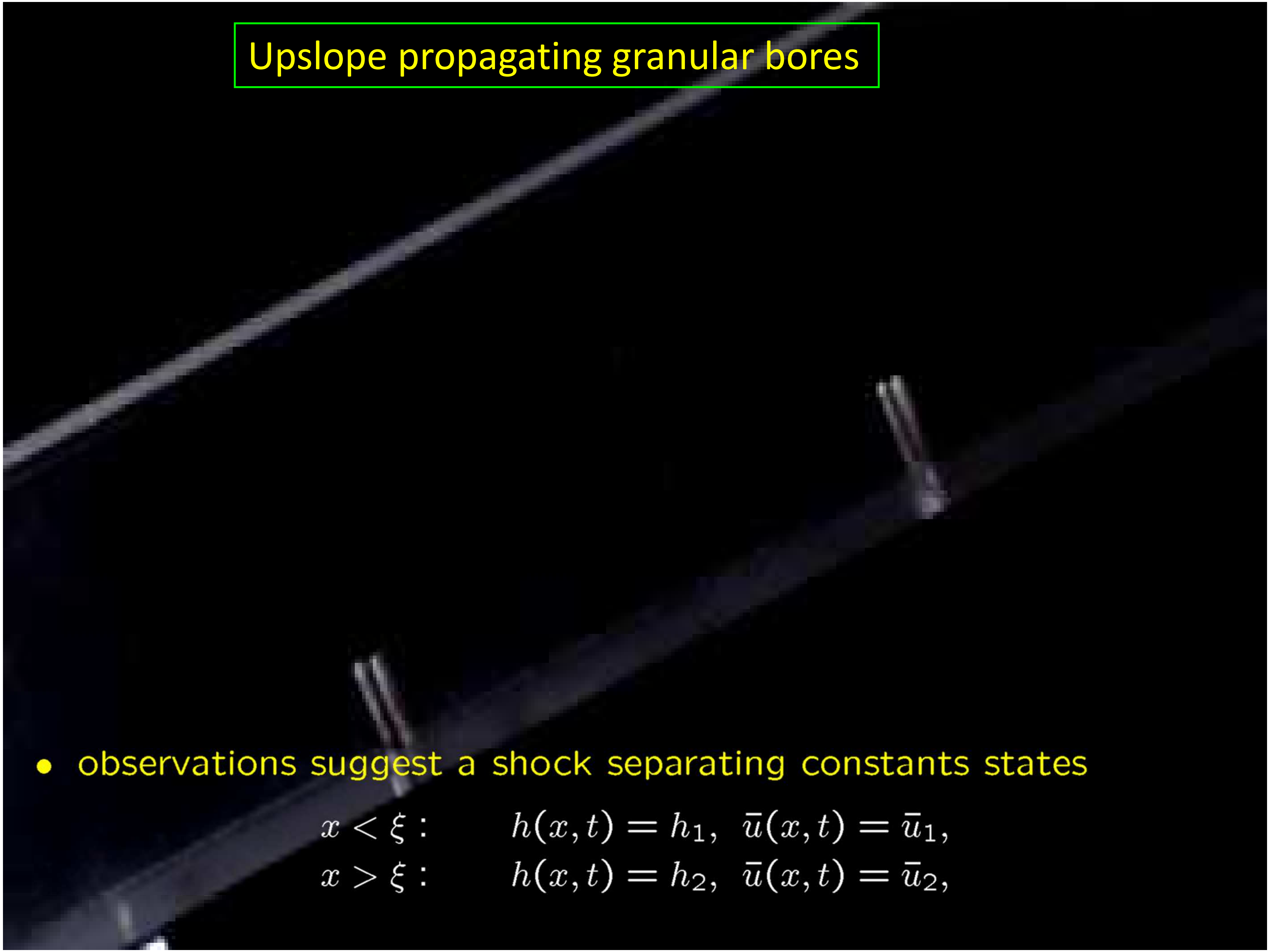

- observations suggest a shock separating constants states

$$x < \xi : \qquad h(x,t) = h_1,\ \ \bar{u}(x,t) = \bar{u}_1,$$
$$x > \xi : \qquad h(x,t) = h_2,\ \ \bar{u}(x,t) = \bar{u}_2,$$

- At shocks the mass and momentum jump conditions are

$$
\begin{aligned}
[\![h(\bar{u} - v_n)]\!] &= 0, \\
[\![h\bar{u}(\bar{u} - v_n)]\!] + [\![\tfrac{1}{2} g h^2 \cos\zeta]\!] &= 0,
\end{aligned}
$$

- where v_n is the normal propagation speed and $[\![\cdot]\!]$ is the jump across the discontinuity.
- Assuming the grains come to rest after a bore

$$
v_n = -\sqrt{\frac{h_1}{h_2}\left(\frac{h_1 + h_2}{2}\right) g \cos\zeta}.
$$

- In the lab experiments

$$
h_1 = 0.61\,\text{cm}, \qquad h_2 = 7.29\,\text{cm} \qquad \Rightarrow v_n = -16.99\,\text{cm/s}
$$

- lies within 10% of the measured value of $v_n = -15.4\,\text{cm/s}$

Gray, Tai & Noelle (2003) *J. Fluid Mech.* **491**, 161-181.

Proposed defence for the Schneefernerhaus, Zugspitze

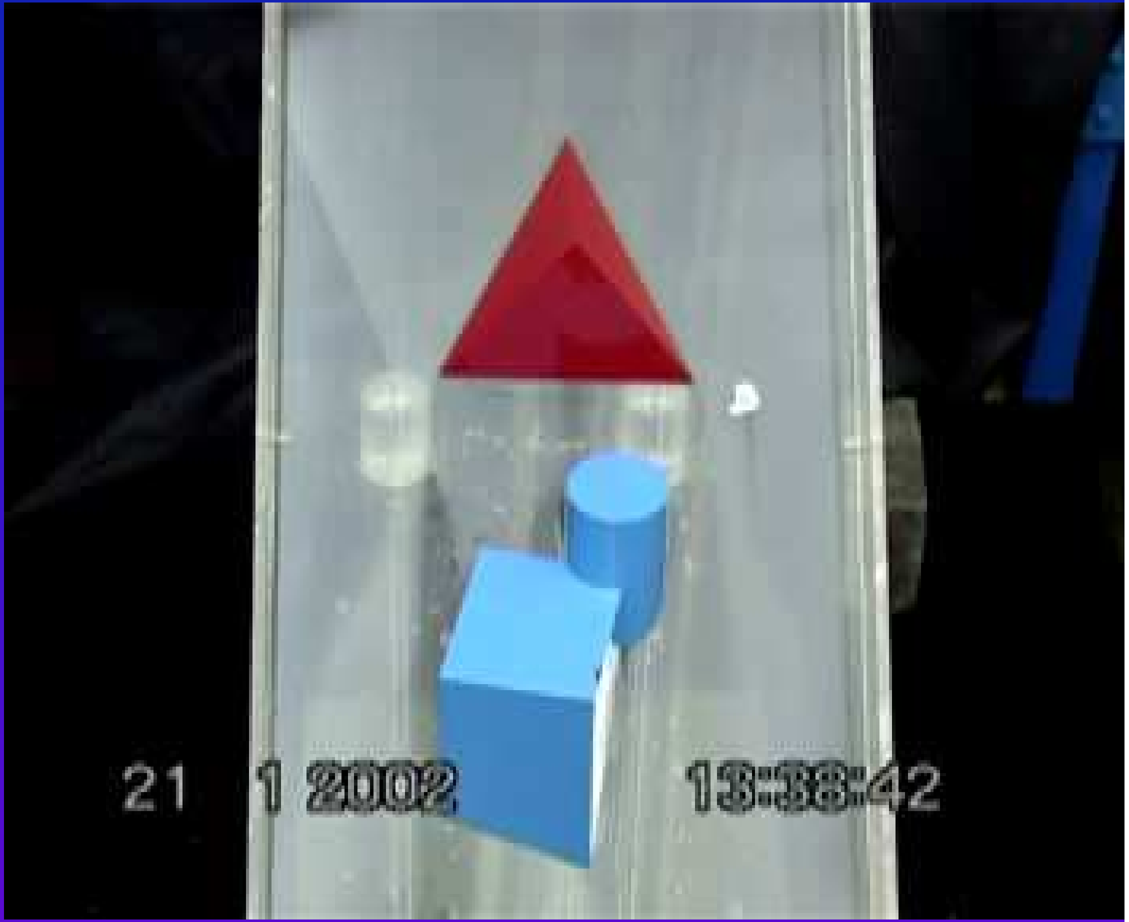

- Use avalanche model to compute the flow past obstacles

Two-dimensional depth-averaged system

- For avalanche thickness h and mean velocity $\bar{\boldsymbol{u}} = (\bar{u}, \bar{v})$ in the downslope x and cross-slope y directions.

$$
\begin{aligned}
\frac{\partial h}{\partial t} + \frac{\partial}{\partial x}(h\bar{u}) + \frac{\partial}{\partial y}(h\bar{v}) &= 0, \\
\frac{\partial}{\partial t}(h\bar{u}) + \frac{\partial}{\partial x}(h\bar{u}^2) + \frac{\partial}{\partial y}(h\bar{u}\bar{v}) + \frac{\partial}{\partial x}\left(\frac{1}{2}gh^2\cos\zeta\right) &= hgS_{(x)}, \\
\frac{\partial}{\partial t}(h\bar{v}) + \frac{\partial}{\partial x}(h\bar{u}\bar{v}) + \frac{\partial}{\partial y}(h\bar{v}^2) + \frac{\partial}{\partial y}\left(\frac{1}{2}gh^2\cos\zeta\right) &= hgS_{(y)},
\end{aligned}
$$

- source terms composed of gravity, basal friction μ and gradients of the basal topography b

$$
\begin{aligned}
S_{(x)} &= \sin\zeta - \mu(\bar{u}/|\bar{\boldsymbol{u}}|)\cos\zeta - \frac{\partial b}{\partial x}\cos\zeta, \\
S_{(y)} &= -\mu(\bar{v}/|\bar{\boldsymbol{u}}|)\cos\zeta - \frac{\partial b}{\partial y}\cos\zeta,
\end{aligned}
$$

Grigorian *et al.* 1967; Gray *et al.* P. Roy. Soc. 1999, JFM 2003

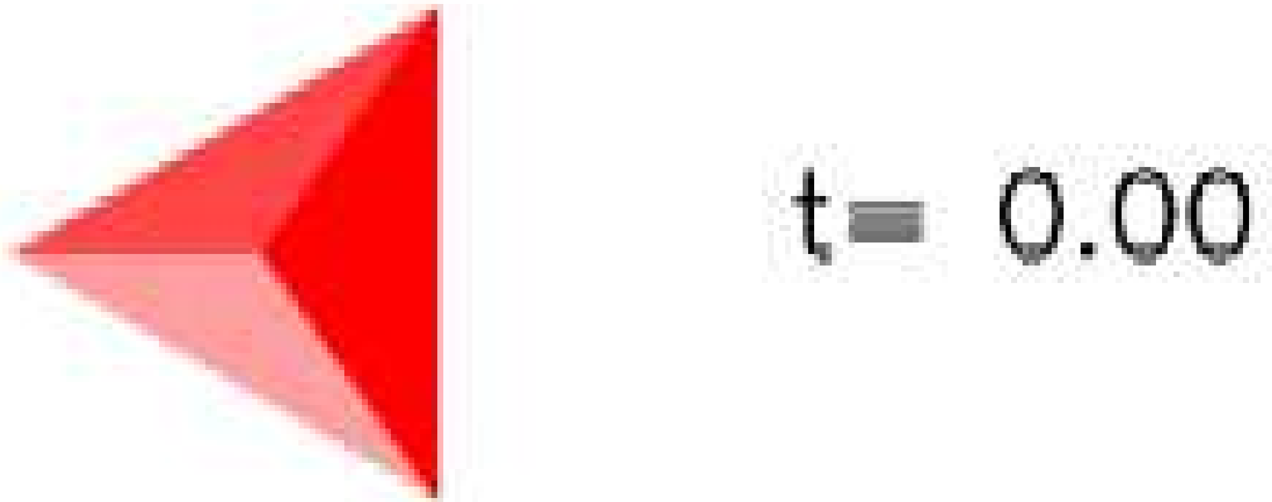

Gray, Tai & Noelle (2003) *J. Fluid Mech.* **491**, 161-181.

Weak, strong and detached oblique shocks

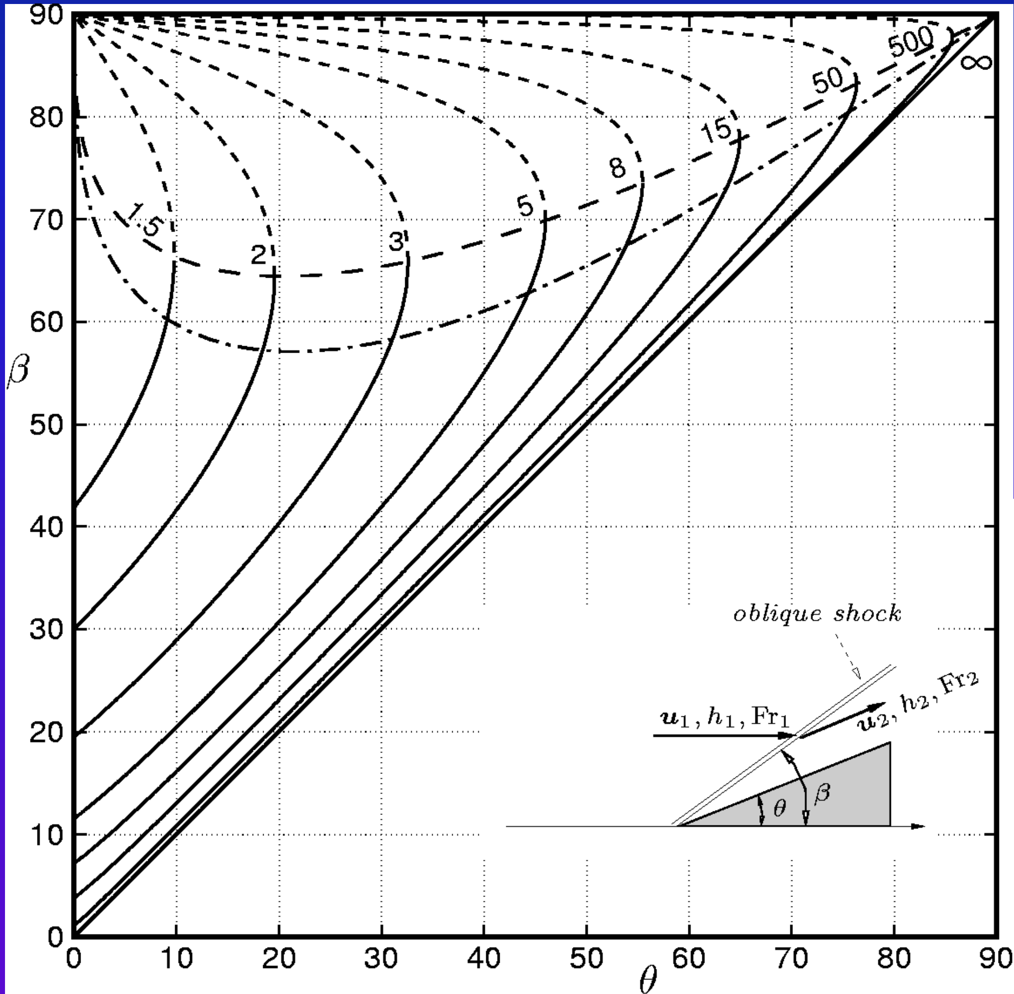

$$\tan\theta = \frac{\tan\beta\left(\sqrt{1+8\mathrm{Fr}_1^2\sin^2\beta}-3\right)}{2\tan^2\beta-1+\sqrt{1+8\mathrm{Fr}_1^2\sin^2\beta}}.$$

Gray & Cui (2007) *J. Fluid Mech.* **579**, 113-136.

$Fr_1 = 5$, $\theta = 20°$, $\zeta = 38°$

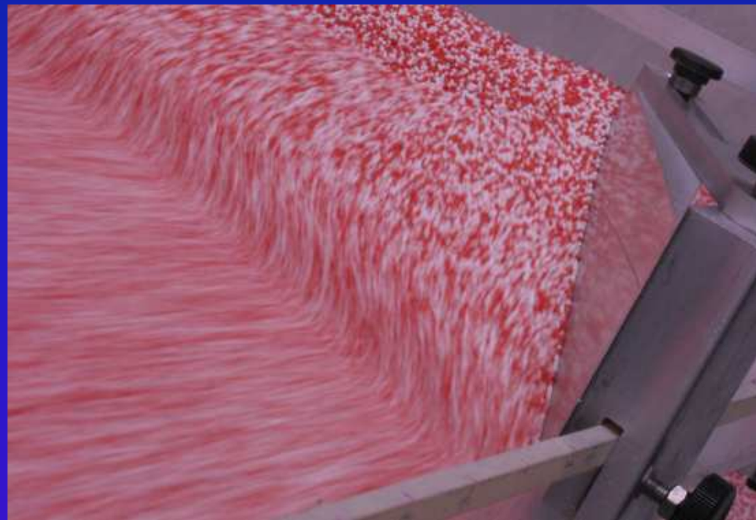

$\beta_s = 86.2°$ $(78° \pm 2°)$

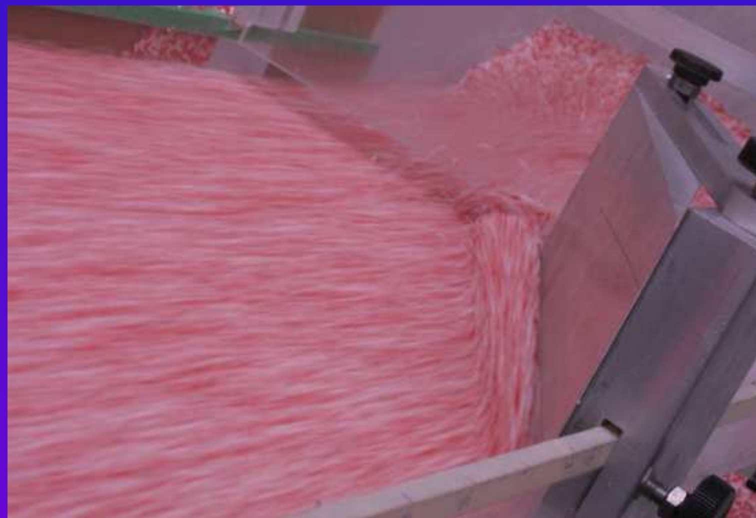

$\beta_w = 30.7°$ $(29° \pm 1°)$


Weak Oblique Shock


Strong Oblique Shock

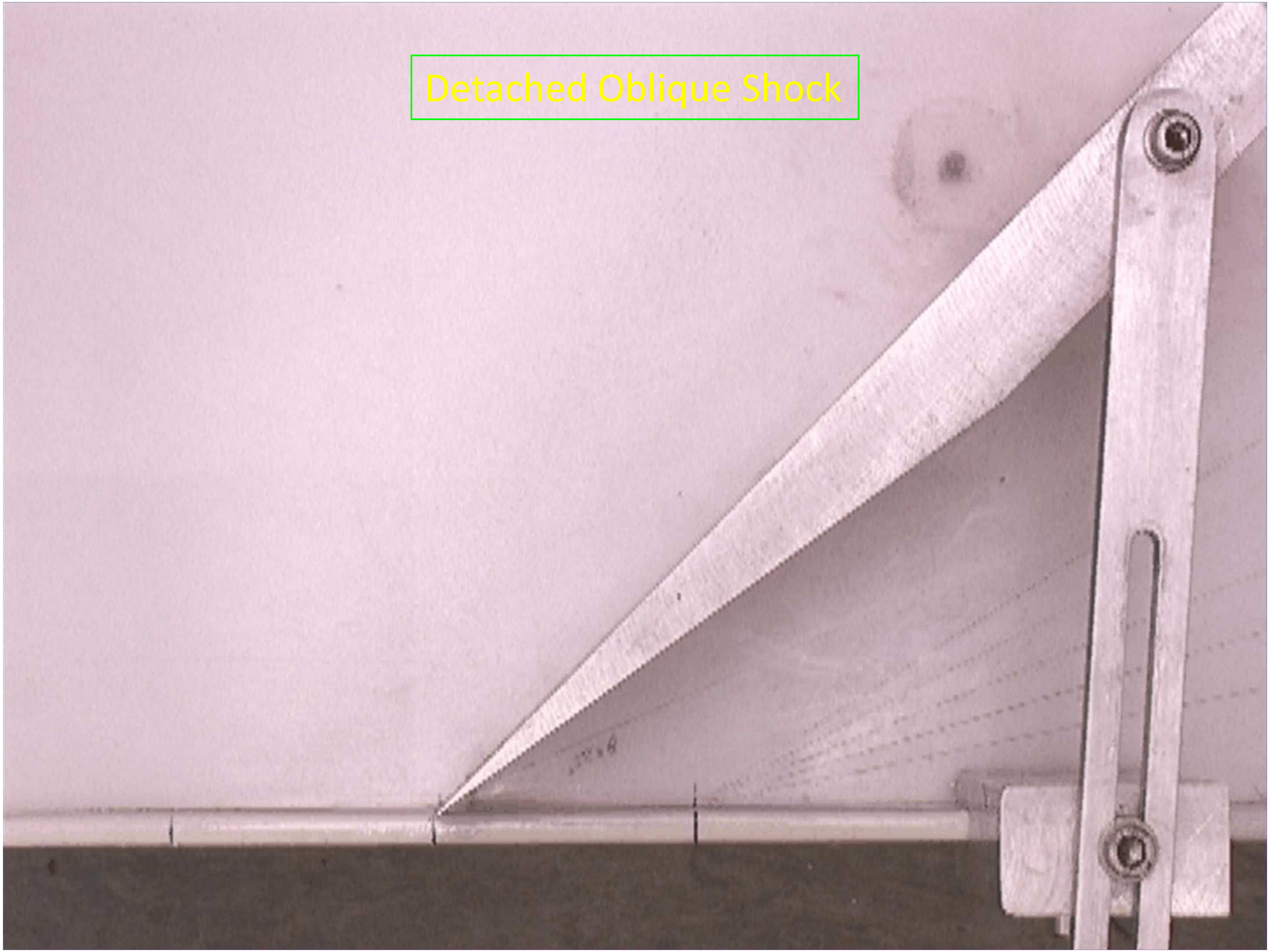
Detached Oblique Shock

Granular jets and hydraulic jumps on an inclined plane

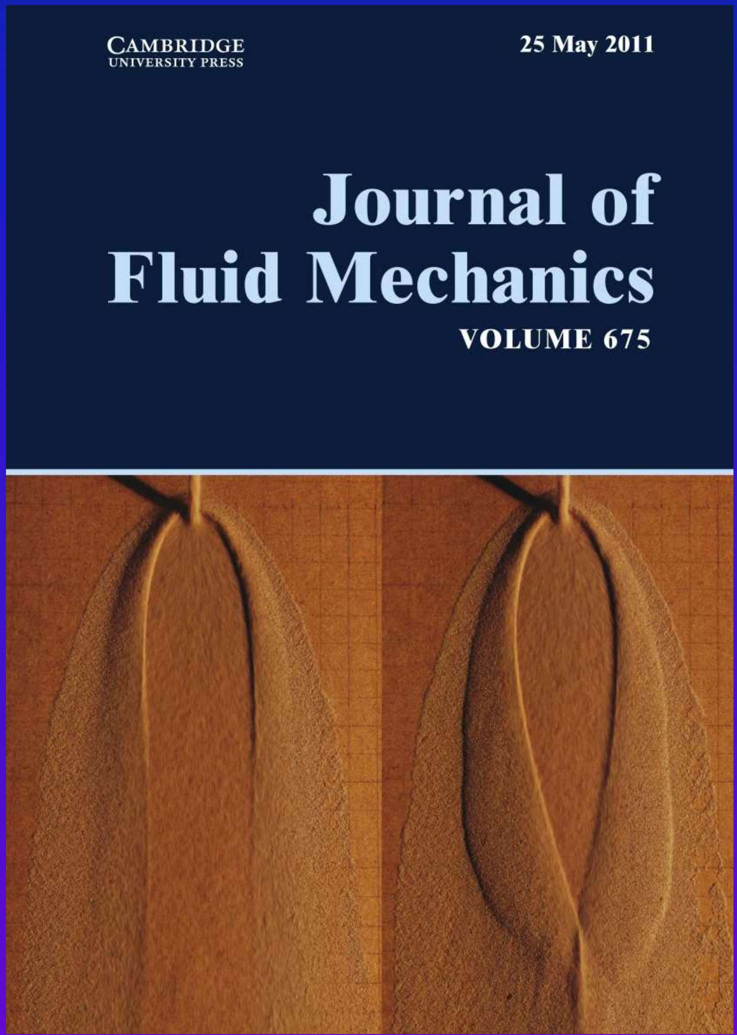

- Oblique impingement of an inviscid jet (Hasson & Peck 1964)
- Friction law for rough beds

$$\mu = \tan\zeta_1 + \frac{\tan\zeta_2 - \tan\zeta_1}{1 + \beta h/(\mathcal{L}\mathrm{Fr})},$$

- including treatment of static material for $0 < \mathrm{Fr} < \beta$ (Pouliquen & Forterre 2002)

Johnson & Gray (2011) *J. Fluid Mech.* **675**, 87-116

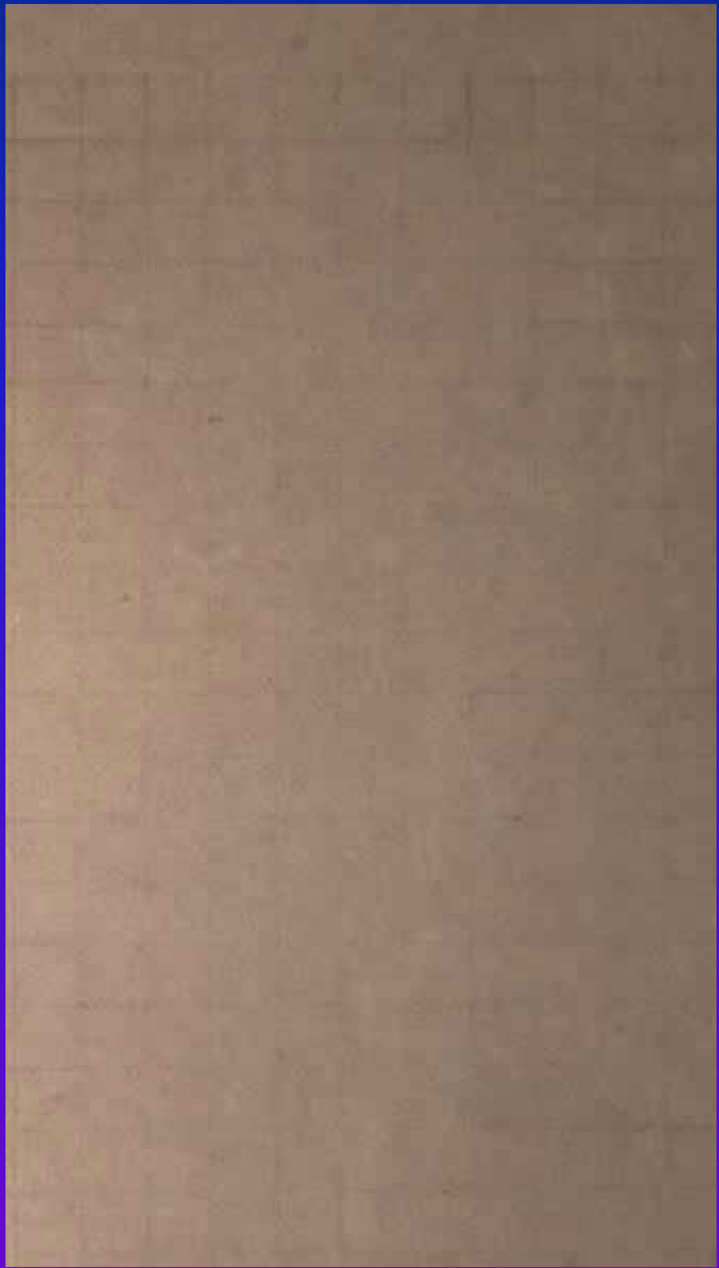

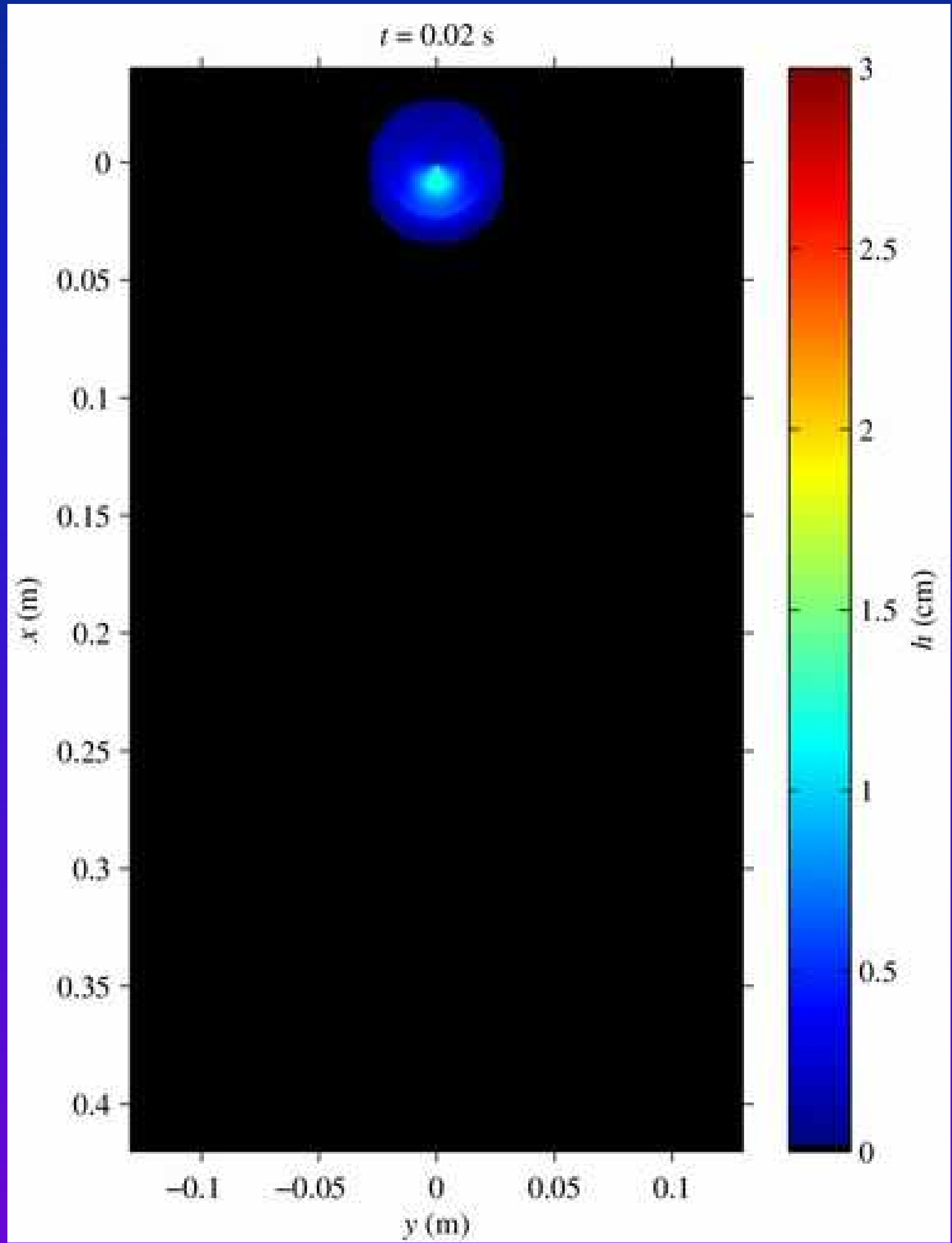

Johnson & Gray (2011) *J. Fluid Mech.* **675**, 87-116

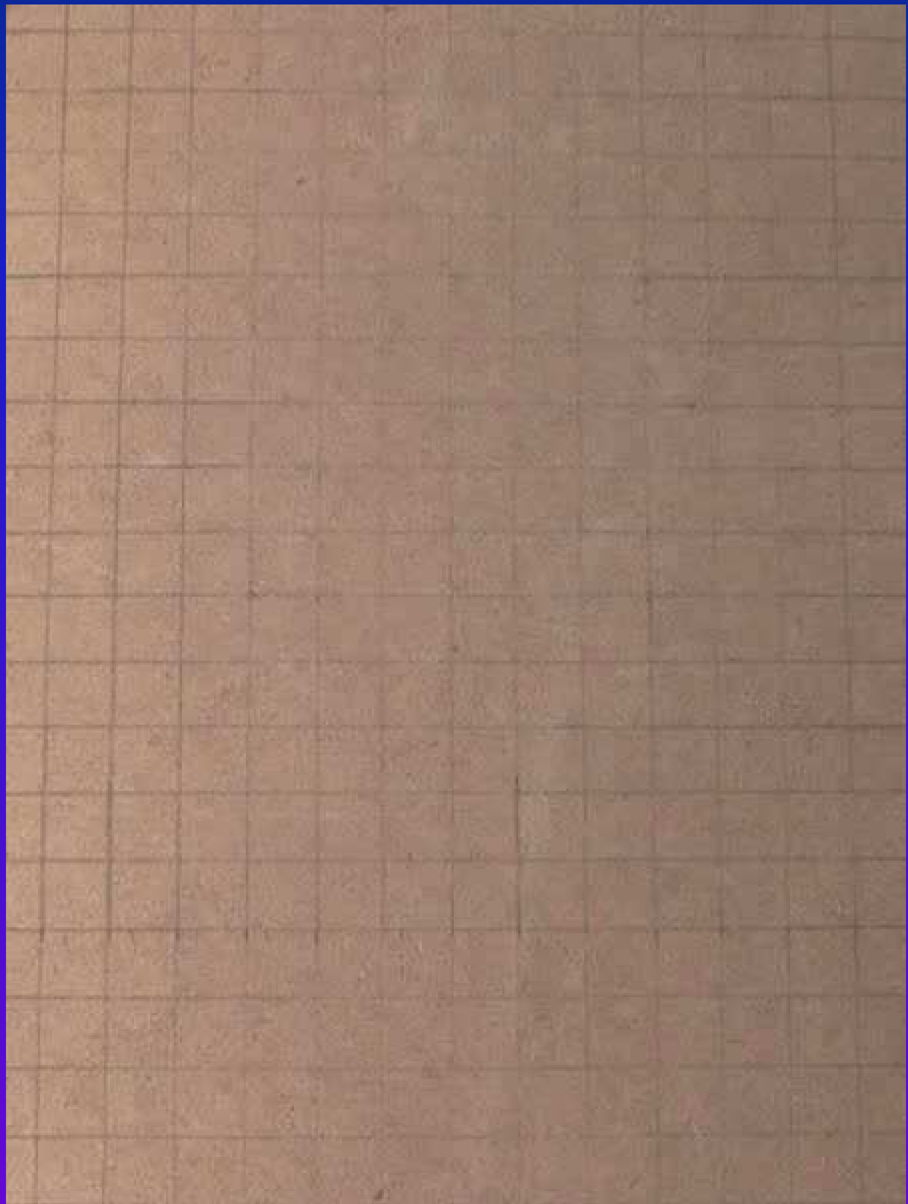

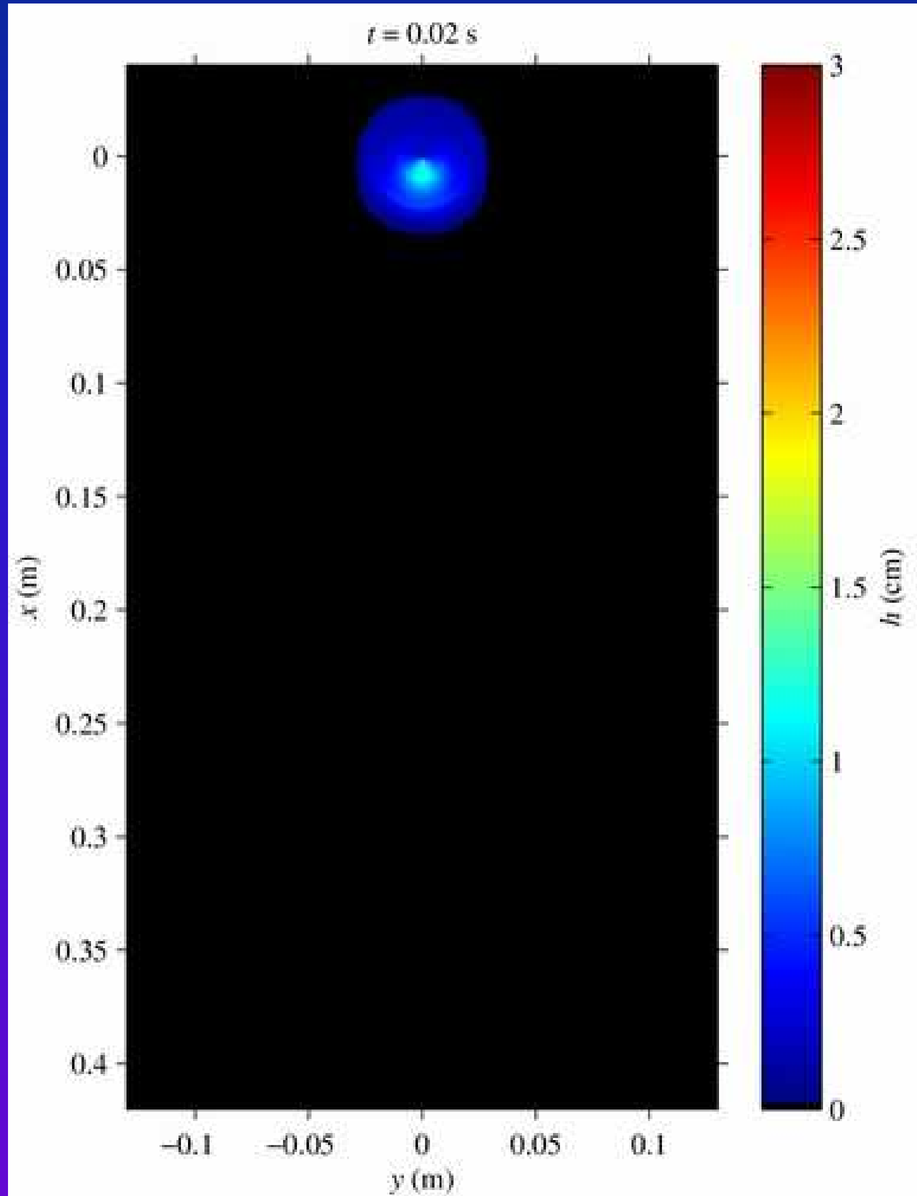

Johnson & Gray (2011) *J. Fluid Mech.* **675**, 87-116

Erosion-deposition waves

- 15^{th} Oct 2000 an unintentional release of 150 000 m^3 water led to a debris flow in Fully Switzerland that had regular surges

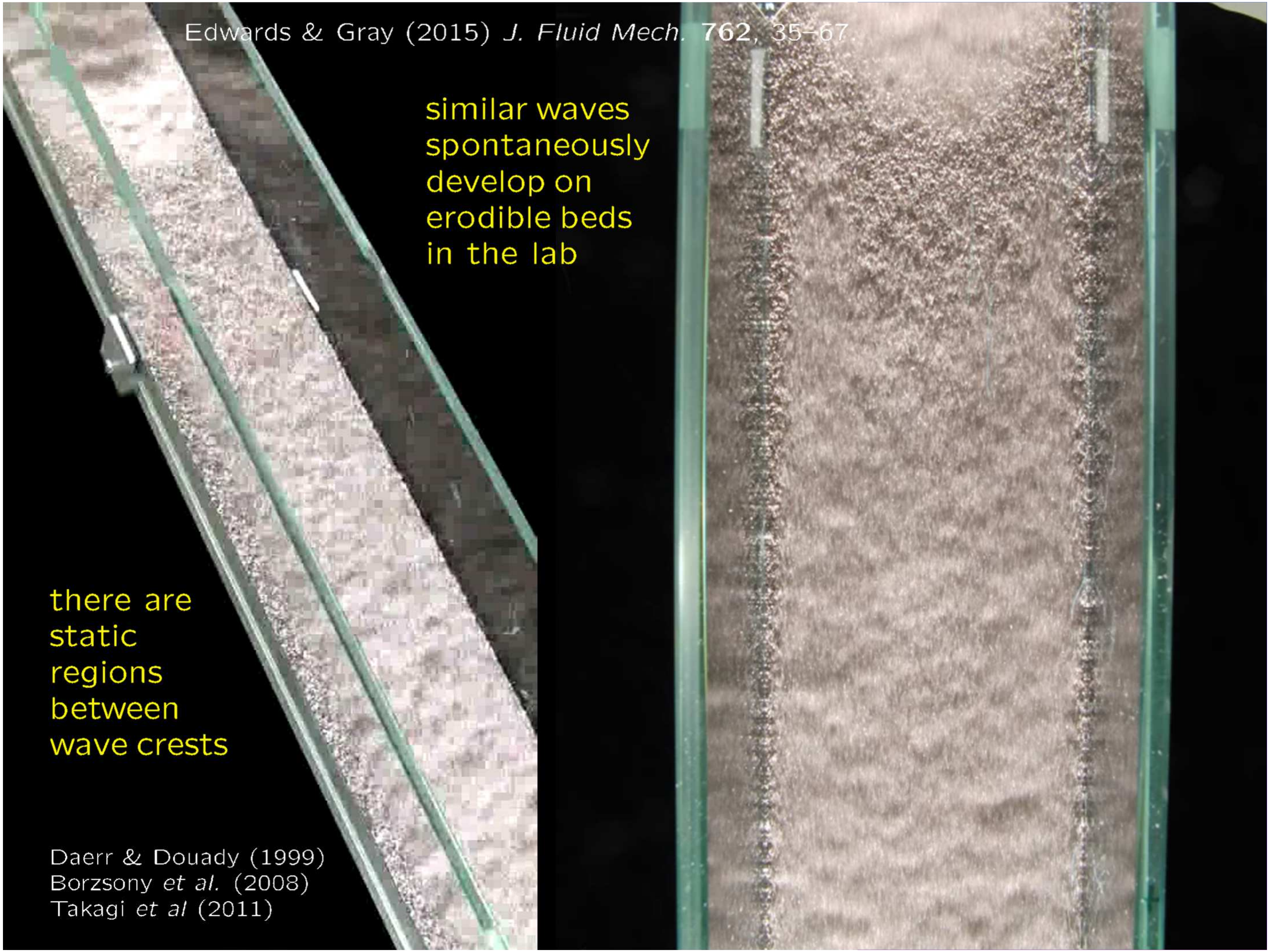
Edwards & Gray (2015) *J. Fluid Mech.* **762**, 35–67.
similar waves spontaneously develop on erodible beds in the lab
there are static regions between wave crests
Daerr & Douady (1999)
Borzsony *et al.* (2008)
Takagi *et al* (2011)

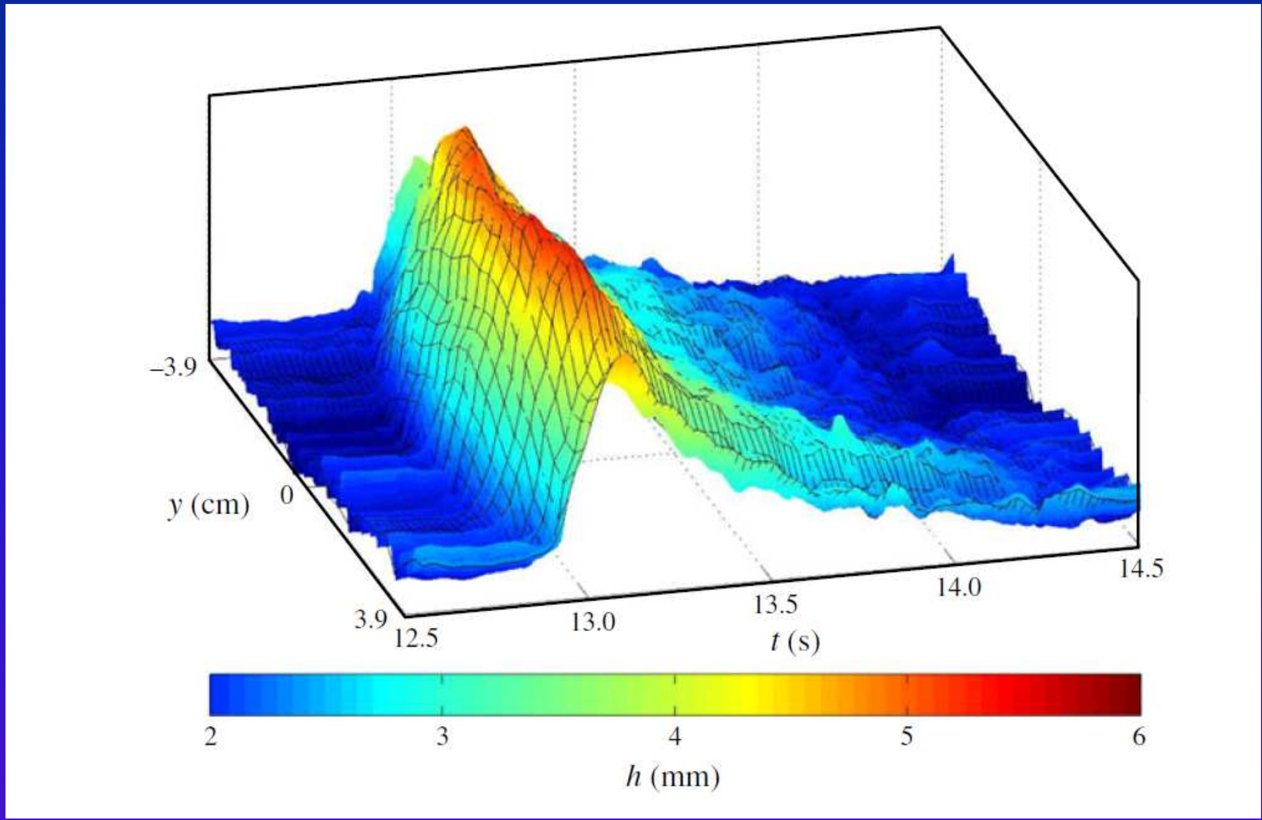

- waves are typically 5mm peak height and have 2mm stationary layer

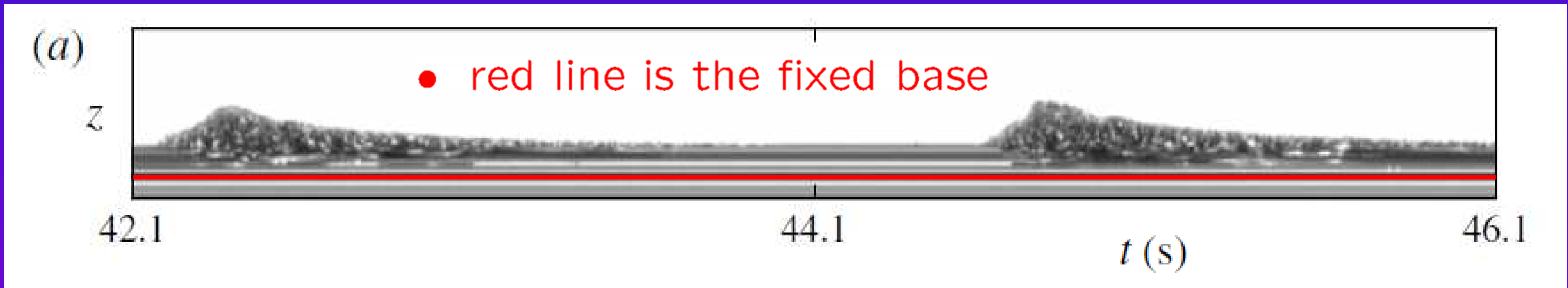

- side-on "photo-finish" shows basal erosion and deposition

Granular solid-fluid phase transition in depth-averaged framework

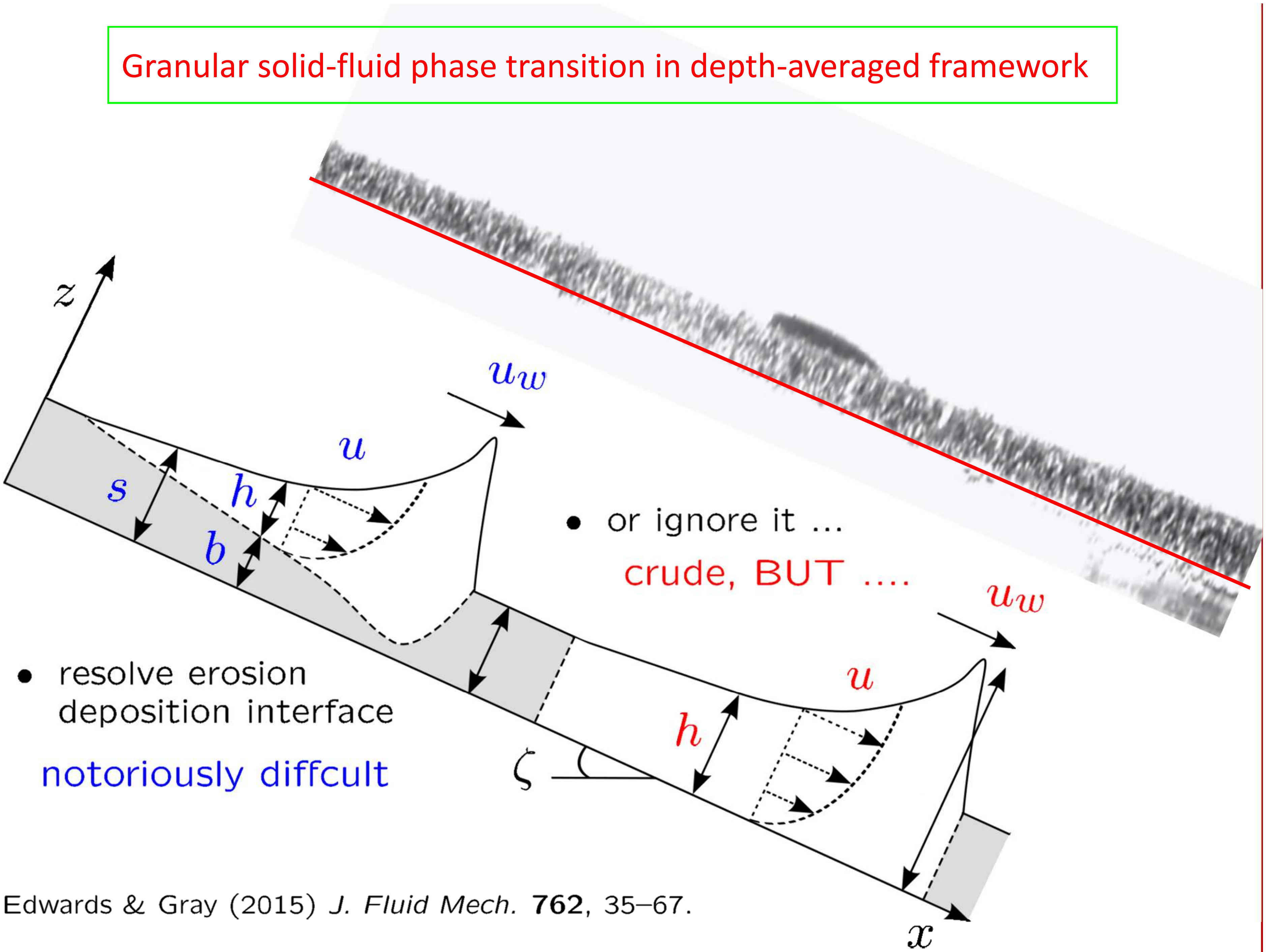

• resolve erosion deposition interface

notoriously diffcult

Edwards & Gray (2015) *J. Fluid Mech.* **762**, 35–67.

Use shallow water avalanche model ...

- Uses shallow water avalanche model (e.g. Grigorian *et al.* 1967, Gray *et al.* 1999, 2003) for the thickness h and the depth-averaged velocity $\bar{u}$

$$\frac{\partial h}{\partial t} + \frac{\partial}{\partial x}(h\bar{u}) = 0$$

$$\frac{\partial}{\partial t}(h\bar{u}) + \frac{\partial}{\partial x}(\chi h\bar{u}^2) + \frac{\partial}{\partial x}\left(\frac{1}{2}h^2 g \cos\zeta\right) = hgS$$

- where $\chi = \overline{u^2}/\bar{u}^2$ is the shape factor, g is the constant of gravitational acceleration and the source term

$$S = \sin\zeta - \mu\frac{\bar{u}}{|\bar{u}|}\cos\zeta$$

- consists of gravitational acceleration and basal fiction μ

Grigorian, Eglit & Iakimov (1967), *Tr. Vysokokogornogo Geofizich Inst.* **12**, 104-113.
Gray, Wieland & Hutter (1999) *Proc. Roy. Soc. A* **455**, 1841-1874
Gray, Tai & Noelle (2003) *J. Fluid Mech.* **491**, 161-181

Pouliquen & Forterre (2002)

- Measured basal friction by determining the thickness as which the grains
  - came to rest
  - when they started moving again from a static state

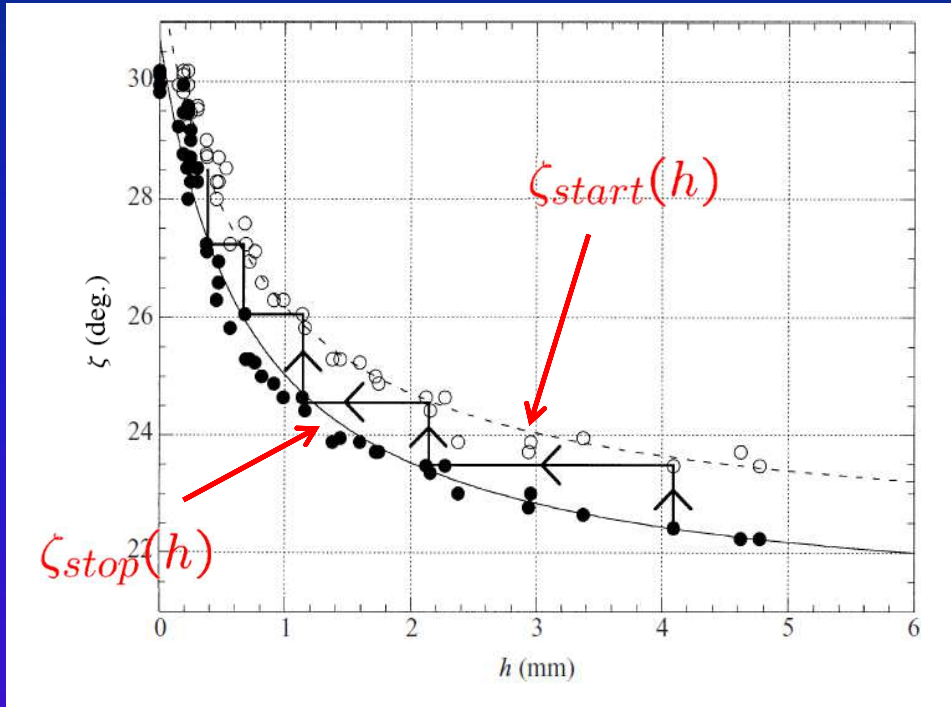

- gave effective basal friction law

$$\mu(h,\mathrm{Fr}) = \begin{cases} \mu_1 + \dfrac{\mu_2-\mu_1}{1+h\beta/(L\mathrm{Fr})}, & \mathrm{Fr} \geq \beta, \quad \text{dynamic} \\ \left(\dfrac{\mathrm{Fr}}{\beta}\right)^{\kappa}(\mu_1-\mu_3)+\mu_3+\dfrac{\mu_2-\mu_1}{1+h/L}, & 0<\mathrm{Fr}<\beta, \quad \text{intermediate} \\ \mu_3 + \dfrac{\mu_2-\mu_1}{1+h/L}, & \mathrm{Fr}=0, \quad \text{static} \end{cases}$$

- where Fr is the Froude number, $\kappa = 10^{-3}$ and $\mu_1 = \tan\zeta_1$, $\mu_2 = \tan\zeta_2$ and $\mu_3 = \tan\zeta_3$ are the tangents of the angles, ζ_1, ζ_2 and ζ_3.

Pouliquen & Forterre (2002) *J. Fluid Mech.* **453**, 133-151.

Travelling-wave solutions in the absence of viscosity

- In a frame travelling at speed u_w with coordinates

$$\xi = x - u_w t, \qquad \tau = t.$$

- Assuming $\partial/\partial\tau = 0$ and $\chi = 1$ the system reduces to

$$\frac{\mathrm{d}}{\mathrm{d}\xi}\left(h(\bar{u} - u_w)\right) = 0,$$

$$h(\bar{u} - u_w)\frac{\mathrm{d}\bar{u}}{\mathrm{d}\xi} + hg\cos\zeta\frac{\mathrm{d}h}{\mathrm{d}\xi} = hg\cos\zeta(\tan\zeta - \mu)$$

- Since $\bar{u} = 0$ in a stationary layer of thickness $h = h_+$

$$h(\bar{u} - u_w) = -h_+ u_w \qquad \Rightarrow \qquad \bar{u} = u_w\left(1 - \frac{h_+}{h}\right).$$

- The flow thickness for which $\mathrm{Fr} = \beta$ is now defined as $h = h_\star$

$$\Rightarrow \qquad u_w = \frac{\beta h_\star^{3/2}\sqrt{g\cos\zeta}}{h_\star - h_+}.$$

Edwards & Gray (2015) *J. Fluid Mech.* **762**, 35-67.

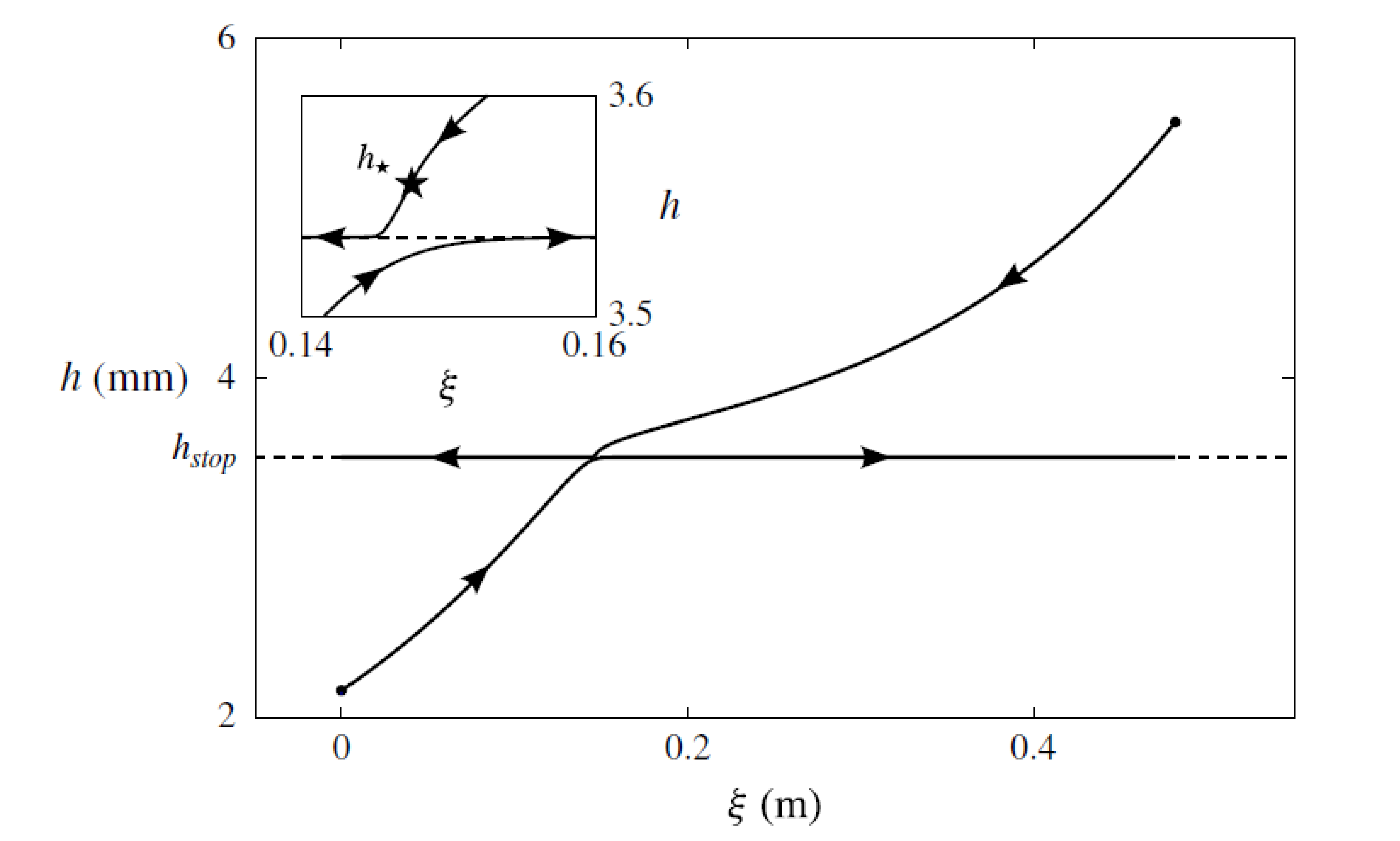

- Integration of the first order ODE indicates a problem
- solution asymptotes to a critical thickness $h_* \gg h_{crit} > h_{stop}$
- To get through this point, ones needs a little bit of viscosity

Edwards & Gray (2015) *J. Fluid Mech.* **762**, 35-67.

The μ(I)-rheology for liquid-like granular flows

- GDR MIDI (2004) and Jop *et al.* (2006): proposed constitutive law

$$\boldsymbol{\tau} = \mu(I) p \frac{\boldsymbol{D}}{||\boldsymbol{D}||}$$

- where 2nd invariant

$$||\boldsymbol{D}|| = \sqrt{\frac{1}{2}\mathrm{tr}\boldsymbol{D}^2}$$

- If $\mu =$ const this reduces to Mohr-Coulomb law

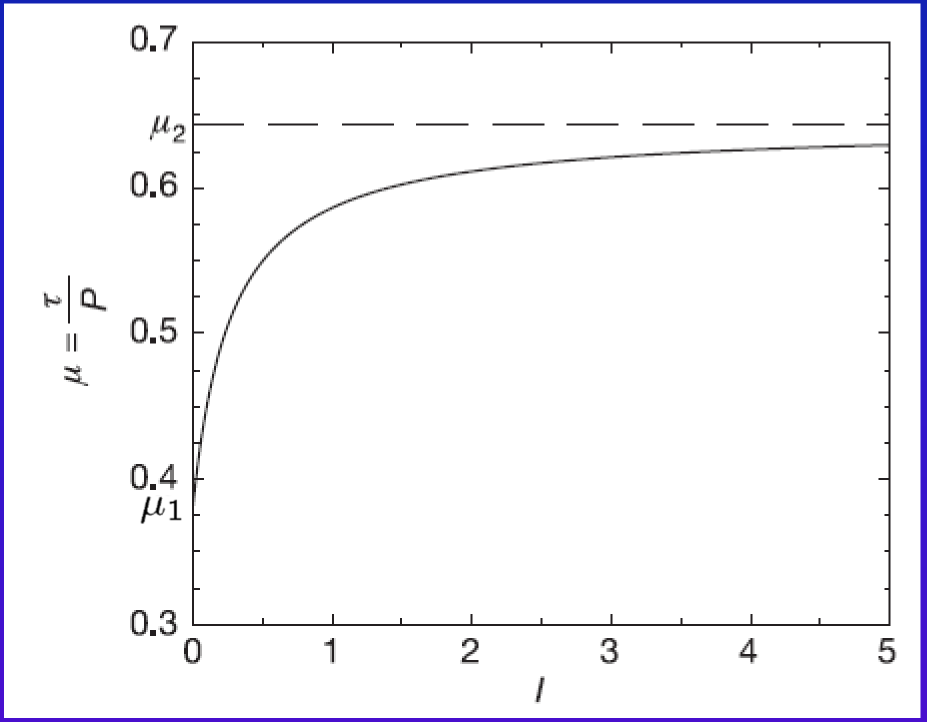

- BUT, friction μ is a function of the inertial number I

$$\mu(I) = \mu_1 + \frac{\mu_2 - \mu_1}{I_0/I + 1}, \qquad I = \frac{2||\boldsymbol{D}||d}{\sqrt{p/\rho^*}},$$

- where d is the particle diameter and ρ^* is the intrinsic density.

The Continuum Sand-Glass

Solver: We apply the Open-source Gerris (Popinet 2003)
http://gfs.sourceforge.net
(incompressible Navier-Stokes equations using a VOF method) (Popinet 2003, 2009)

$$\begin{aligned}
\boldsymbol{\nabla}.\boldsymbol{u} &= 0 \\
\rho\left(\frac{\partial \boldsymbol{u}}{\partial t} + \boldsymbol{u}.\boldsymbol{\nabla}\boldsymbol{u}\right) &= -\boldsymbol{\nabla}p + \boldsymbol{\nabla}.(2\eta\boldsymbol{D}) + \rho\boldsymbol{g} \\
\frac{\partial c}{\partial t} + \boldsymbol{\nabla}.(c\boldsymbol{u}) &= 0 \\
\rho = c\,\rho_{\text{air}} &+ (1-c)\,\rho_{\text{grains}} \\
\eta = c\,\eta_{\text{air}} &+ (1-c)\,\eta_{\text{grains}}
\end{aligned}$$

⇒ We chose $\rho_{\text{air}} << \rho_{\text{grains}}$
⇒ The free surface is solved in the course of time
⇒ We implement the viscosity:

$$\eta_{\text{grains}} = \min\left(\frac{\mu P}{|\,\dot{\gamma}\,|}, \eta_{max}\right),$$

Lagree, Staron & Popinet 2011

The Continuum Sand-Glass

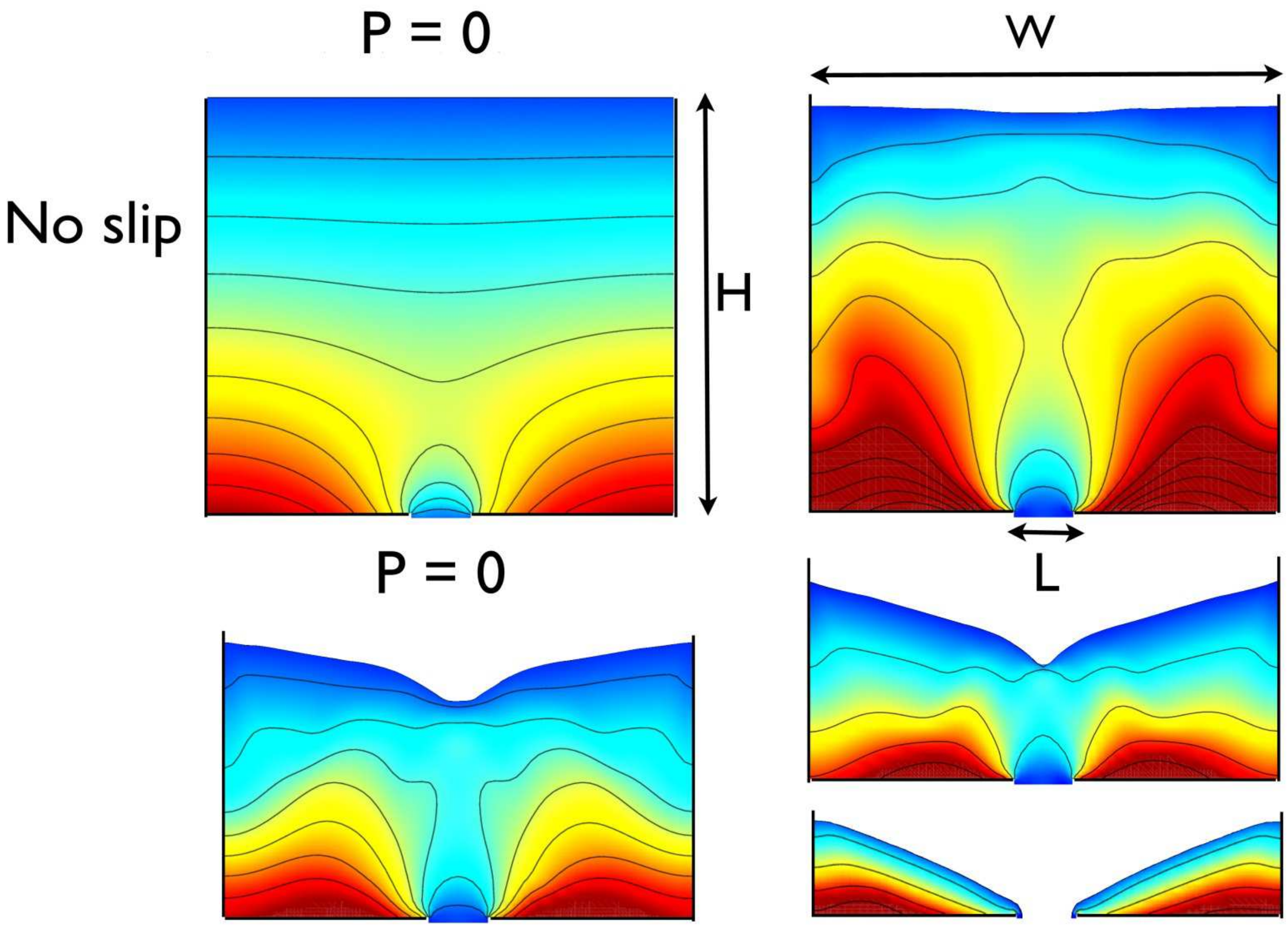

We chose the following value for the rheological parameters:
$\mu_s = 0.32,\ \mu_d = 0.60,\ I_0 = 0.4$

Staron, Lagree & Popinet 2011

The Bagnold solution

- For steady-uniform flow $\boldsymbol{u} = (u(z), 0, 0)$ the normal and downslope momentum balances imply that

$$p = \rho g(h - z)\cos\zeta, \qquad \tau_{xz} = \rho g(h - z)\sin\zeta$$

- Rheology then implies $\mu(I) = \tan\zeta$ and hence I is equal to a constant

$$I_\zeta = I_0\left(\frac{\tan\zeta - \tan\zeta_1}{\tan\zeta_2 - \tan\zeta}\right)$$

- Solve I equation for the downslope velocity

$$u = \frac{2I_\zeta}{3d}\sqrt{\Phi g\cos\zeta}\left(h^{3/2} - (h - z)^{3/2}\right).$$

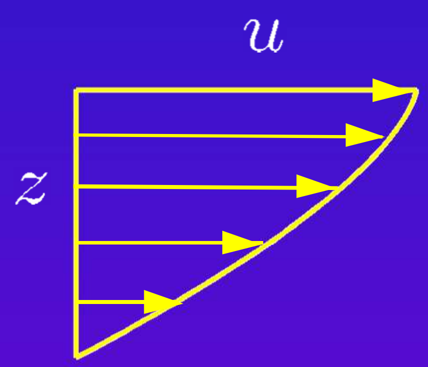

- The depth-averaged Bagnold velocity satisfies

$$\bar{u} = \frac{2I_\zeta}{5d}\sqrt{\Phi g\cos\zeta}\, h^{3/2}$$

The depth-averaged μ(I)-rheology for granular flows

- To first order the inviscid avalanche equations emerge naturally with the dynamic basal friction law

$$\mu_b(h, \mathrm{Fr}) = \mu_1 + \frac{\mu_2 - \mu_1}{\beta h/(L\mathrm{Fr}) + 1}, \qquad \mathrm{Fr} > \beta,$$

- This is just Pouliquen & Forterre's (2002) law, where

$$\mathrm{Fr} = \frac{|\bar{\boldsymbol{u}}|}{\sqrt{gh\cos\zeta}}$$

- Now add in the in-plane deviatoric stress

$$\tau_{xx} = \mu(I)p\frac{D_{xx}}{||\boldsymbol{D}||}$$

- Assume shallow and use Bagnold solution to evaluate

$$D_{xx} = \frac{\partial u}{\partial x}, \qquad ||\boldsymbol{D}|| = \frac{1}{2}\left|\frac{\partial u}{\partial z}\right|$$

- the in-plane deviatoric stress is

$$\tau_{xx} = 2\rho g \sin\zeta \left(h^{1/2}(h-z)^{1/2} - (h-z)\right)\frac{\partial h}{\partial x}.$$

- formal depth-integration gives

$$h\bar{\tau}_{xx} = \frac{1}{3}\rho g \sin\zeta\, h^2 \frac{\partial h}{\partial x}.$$

- Use Bagnold velocity to reformulate

$$h\bar{\tau}_{xx} = \rho \nu h^{3/2}\frac{\partial \bar{u}}{\partial x}$$

- where

$$\nu = \frac{2L\sqrt{g}}{9\beta}\frac{\sin\zeta}{\sqrt{\cos\zeta}}\left(\frac{\tan\zeta_2 - \tan\zeta}{\tan\zeta - \tan\zeta_1}\right).$$

- negative and ill-posed outside range of steady uniform flow

Gray & Edwards (2014) *J. Fluid Mech.* **755**, 503-534.

- Full $\mu(I)$-rheology ill-posed for high and low inertial numbers

Barker *et al.* (2015) *J. Fluid Mech.* **779**, 794–818.

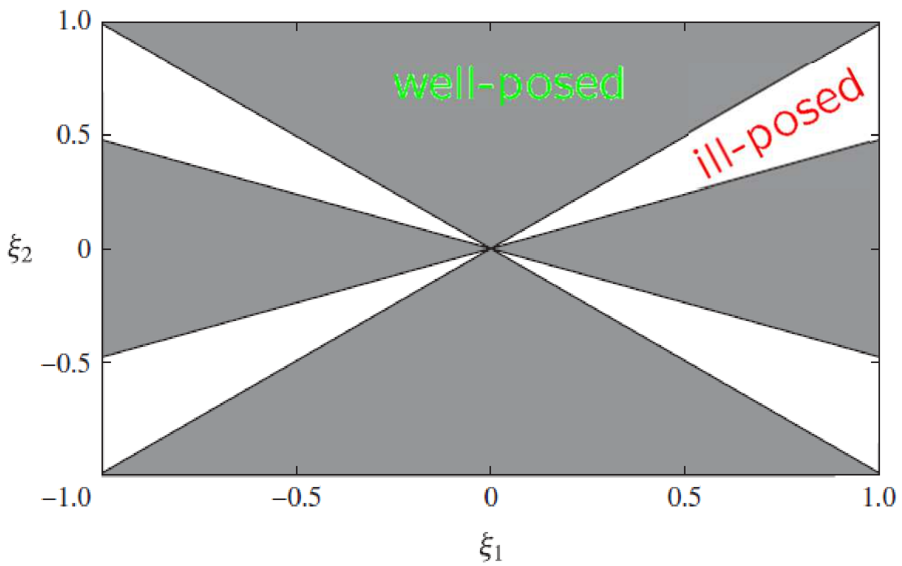

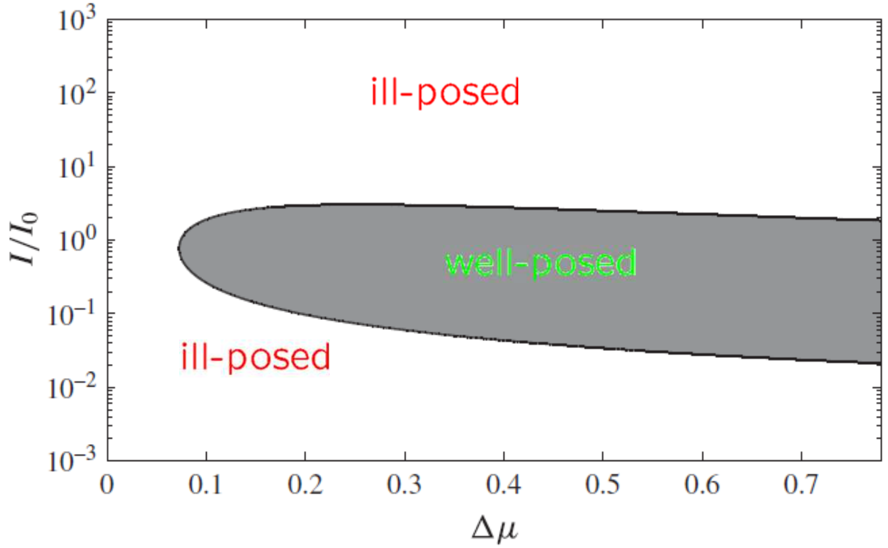

- Small perturbations will grow infinitely quickly in the high wave number limit for certain wave vectors (ξ_1, ξ_2)

$$\left[\begin{array}{c} \hat{\boldsymbol{u}}(\boldsymbol{x},t) \\ \hat{p}(\boldsymbol{x},t) \end{array}\right] = \exp\left(i\boldsymbol{\xi}\cdot\boldsymbol{x} + \lambda t\right)\left[\begin{array}{c} \tilde{\boldsymbol{u}} \\ \tilde{p} \end{array}\right]$$

$$\mu(I) = \mu_1 + \frac{\Delta\mu}{I_0/I + 1}$$

$$I = \frac{2||\boldsymbol{D}||d}{\sqrt{p/\rho^*}}$$

- PRACTICAL IMPLICATION: Two-dimensional transient computations will blow-up in the ill-posed region of parameter space
- In this case for Bagnold flow in the high inertial number regime

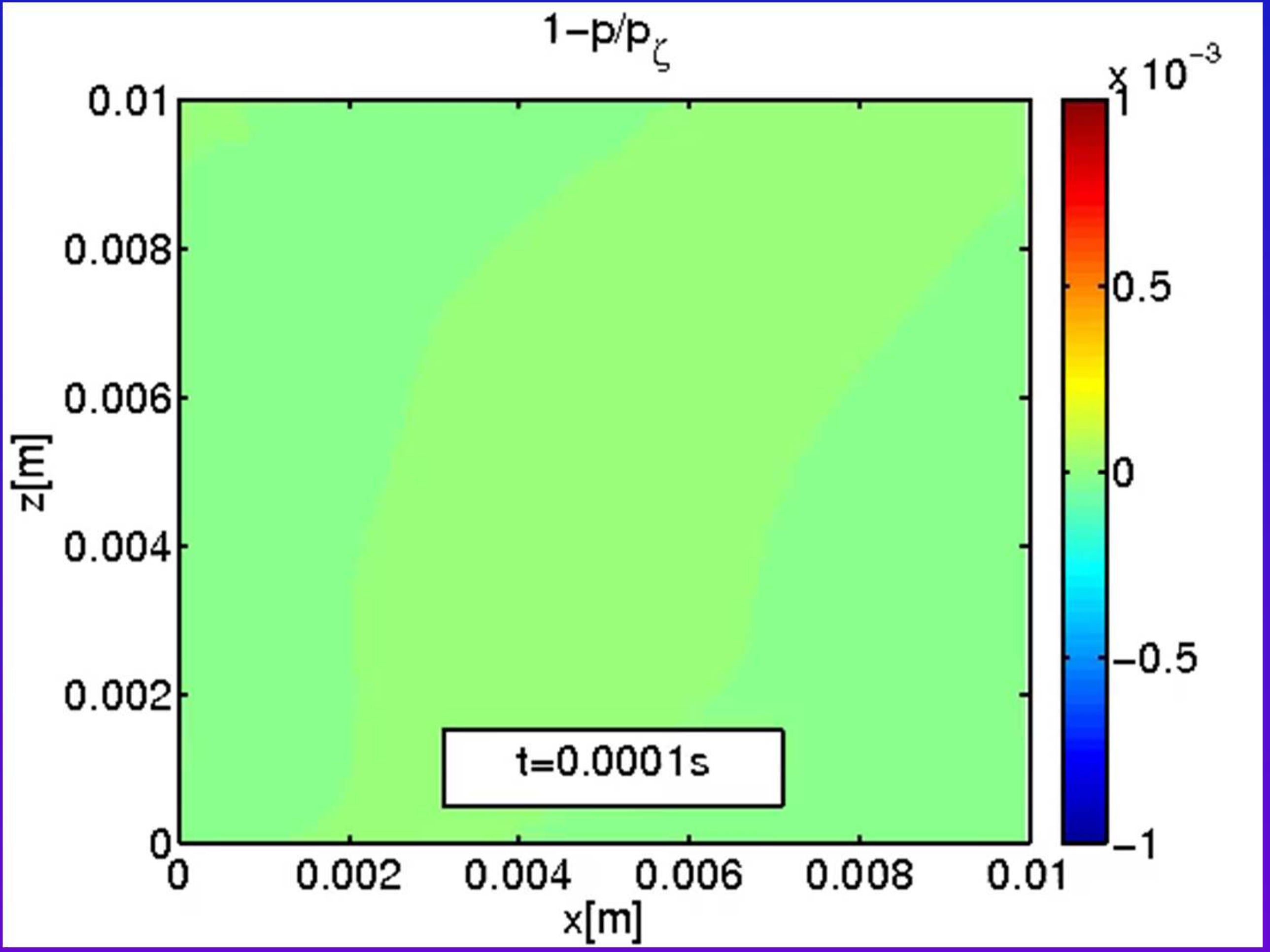

Barker *et al.* (2015) *J. Fluid Mech.* **779**, 794–818.

Application of depth-averaged theory to granular roll-waves

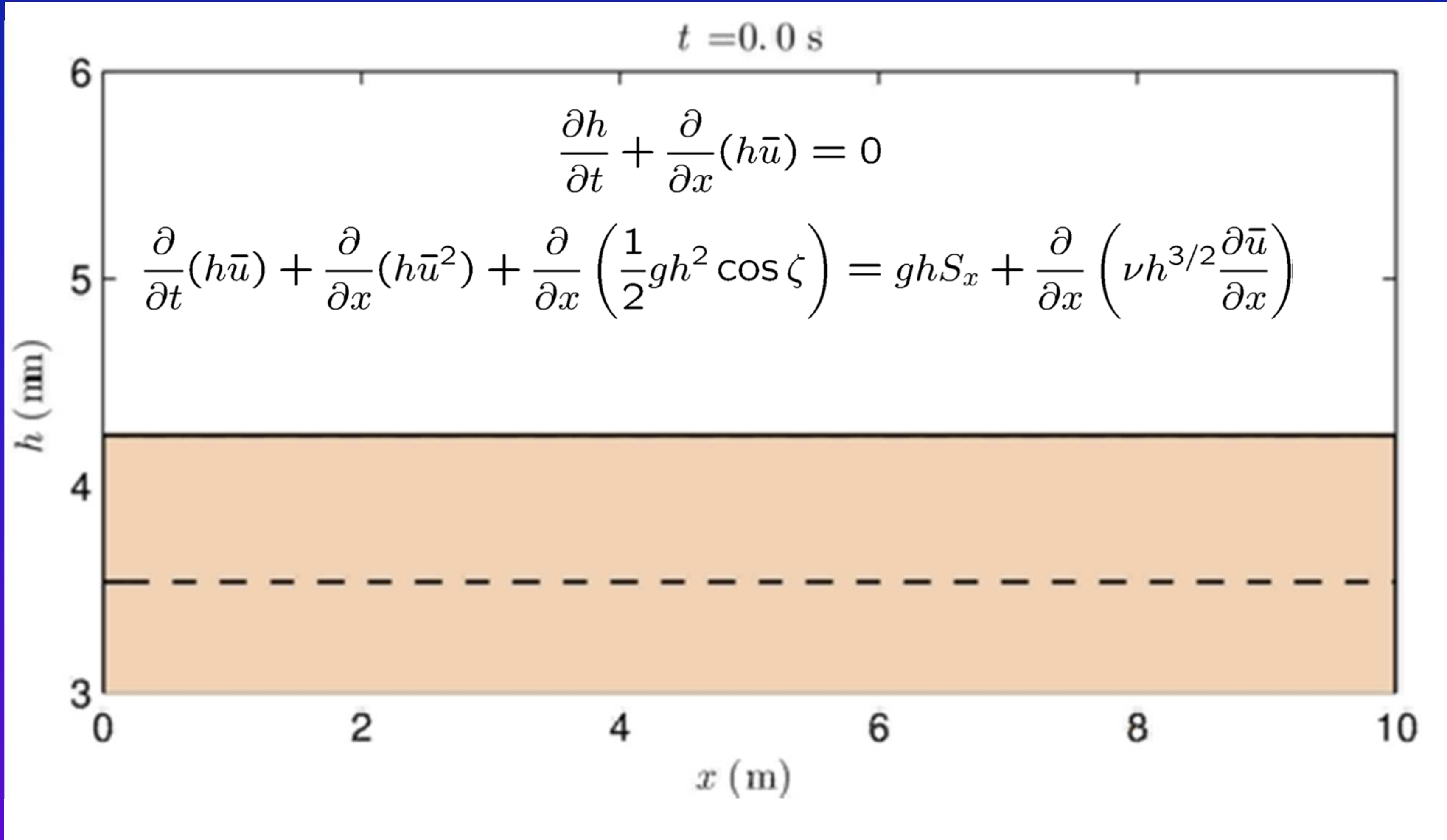

- Adds a singular perturbation to the momentum equation
- This is the only form that is not singular in h or $\bar{u}$

Edwards & Gray (2015) *J. Fluid Mech.* **762**, 35-67.

Measurements of the spatial growth rate of granular roll-waves

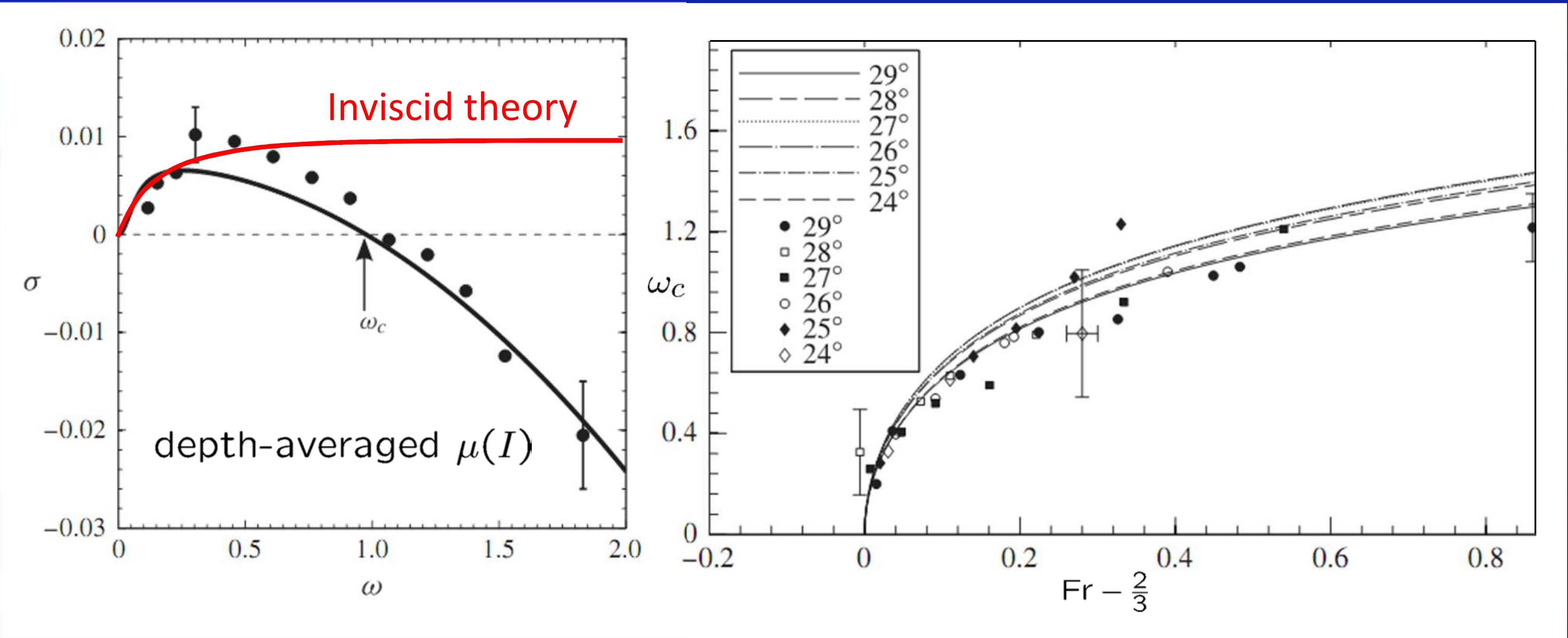

- Forterre & Pouliquen (2003) used loudspeaker to initiate roll waves of a given frequency
- Inviscid theory predicts critical Froude $\mathrm{Fr}_c = 2/3$, but growth occurs at all frequencies ω
- Depth-averaged rheology predicts the cut-off frequency ω_c
- MATCHES WITHOUT ANY FITTING PARAMETERS

Exact travelling wave solutions for roll waves

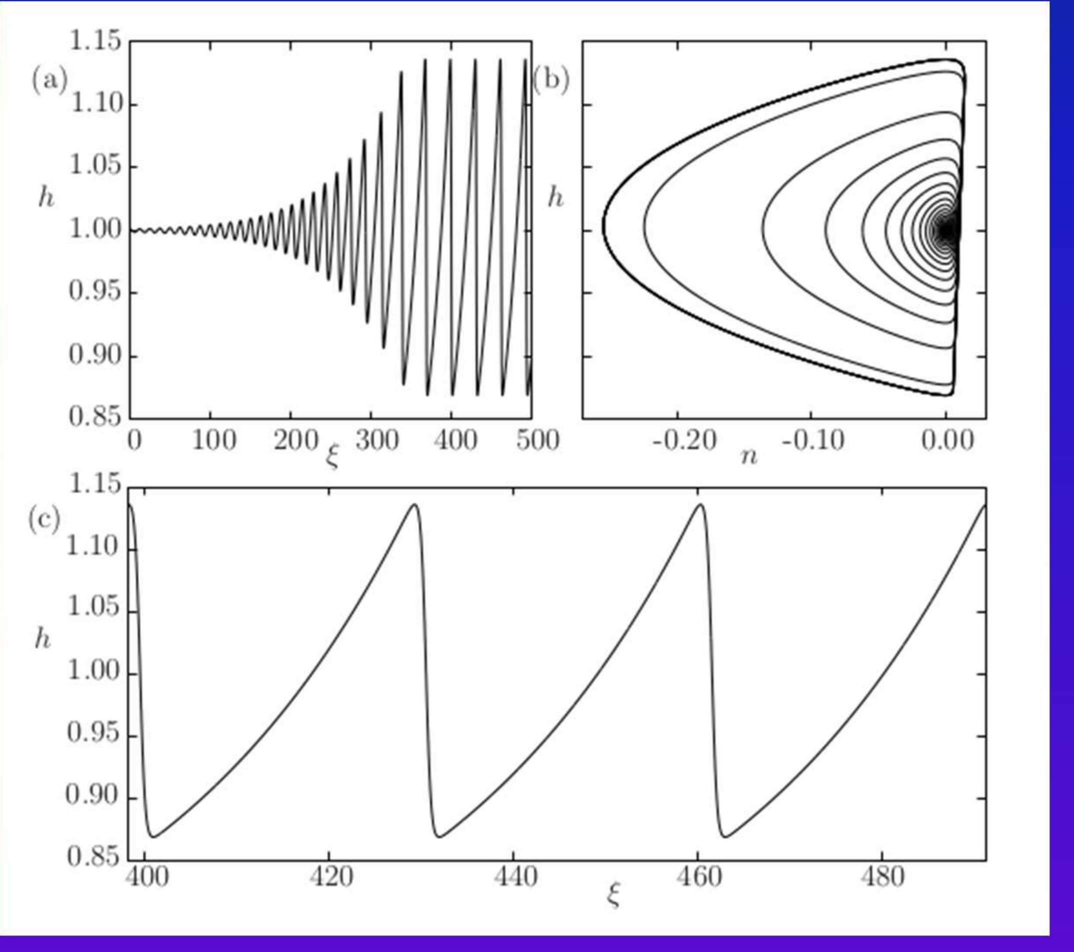

$$n = \frac{dh}{d\xi}$$

- computed by numerically integrating 2nd order ODE with prescribed Fr and u_w until a limit cycle is formed

Gray & Edwards (2014) *J. Fluid Mech.* **755**, 503-534.

Exact travelling wave solutions for erosion-deposition waves

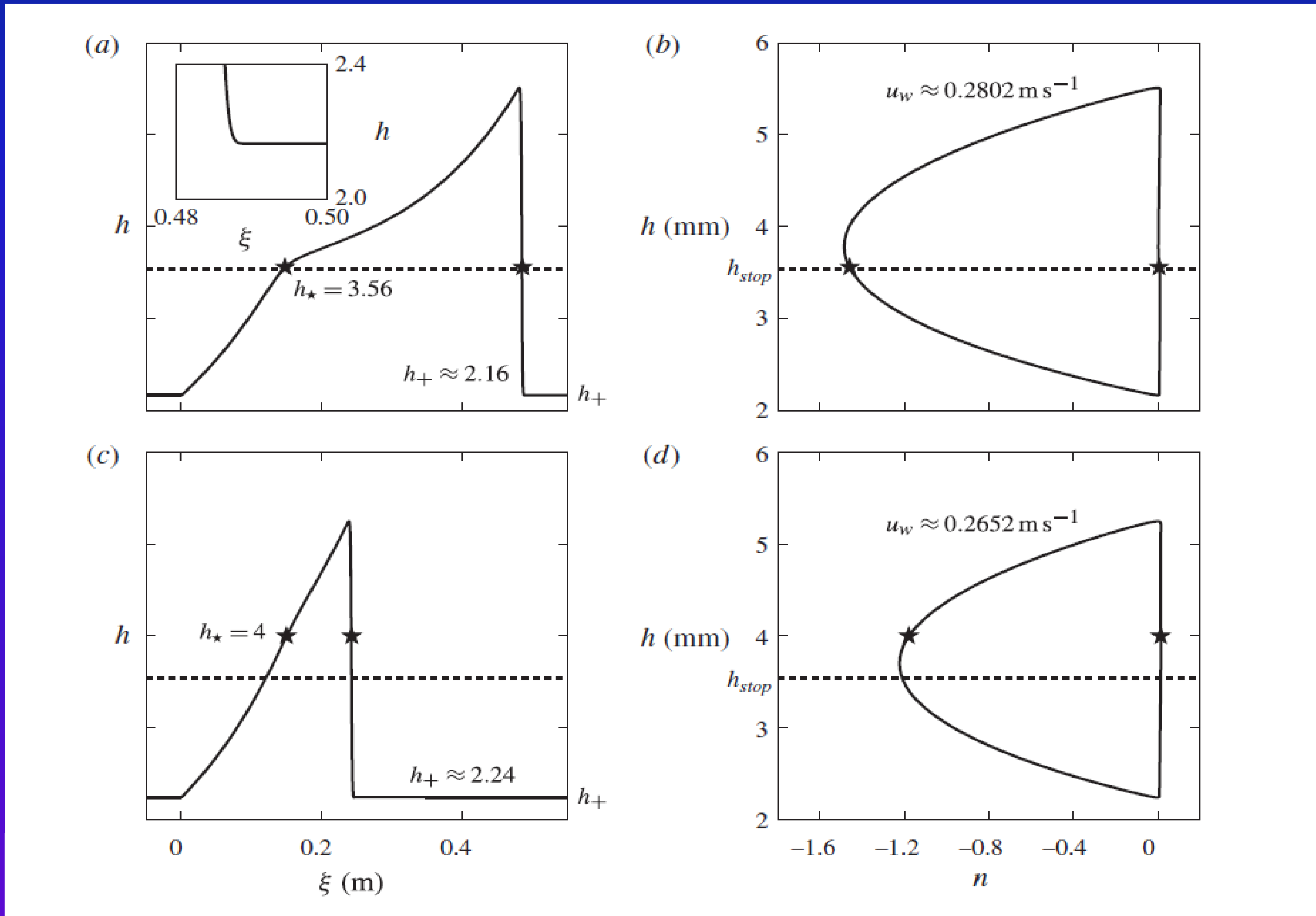

$$n = \frac{dh}{d\xi}$$

- For each solution h_+ and h_* must be prescribed.
- viscosity allows solution to cross the critical line!

Edwards & Gray (2015) *J. Fluid Mech.* **762**, 35-67.

Exact travelling wave solutions for erosion-deposition waves

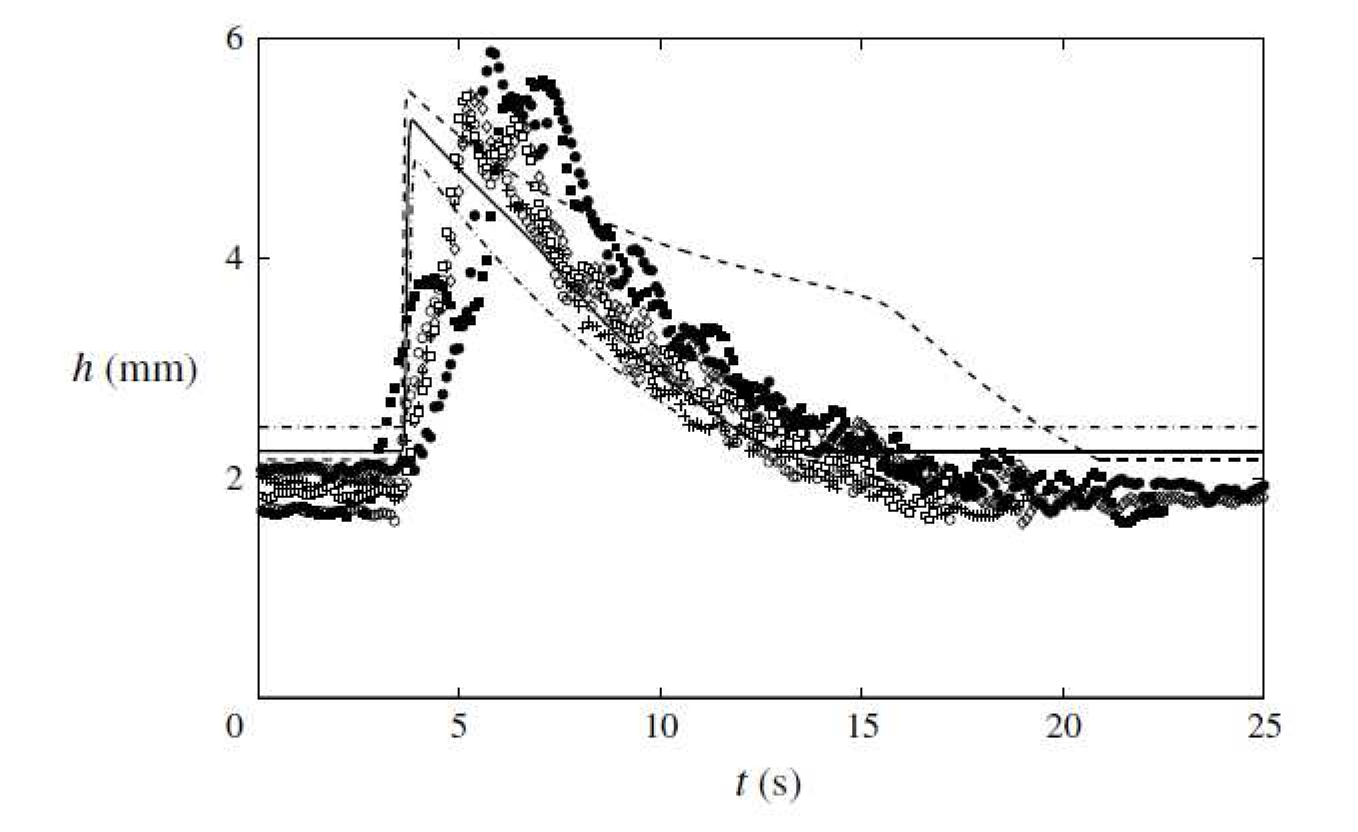

- Exact solution picks off the correct amplitude and wavelength
- ALTHOUGH its shape is a little different
- MAJOR STEP FORWARD in modelling erosion-deposition problems with shallow erodible layers

Edwards & Gray (2015) *J. Fluid Mech.* **762**, 35-67.

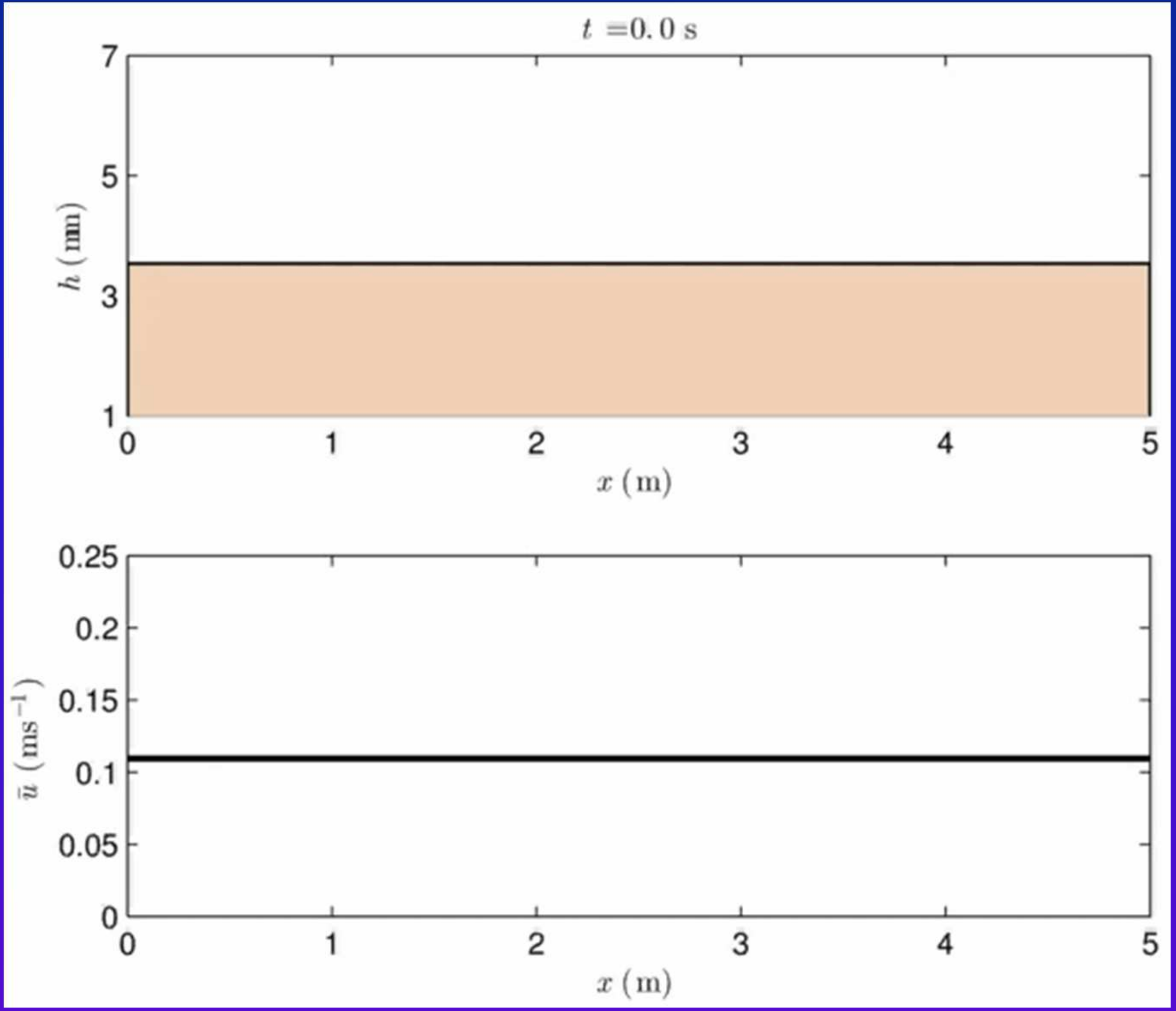

- Numerical solutions with random noise rapidly coarsen into large amplitude waves
- Close to stopping very destructive waves are formed!

Edwards & Gray (2015) *J. Fluid Mech.* **762**, 35-67.

Complex coarsening dynamics is qualitatively reproduced

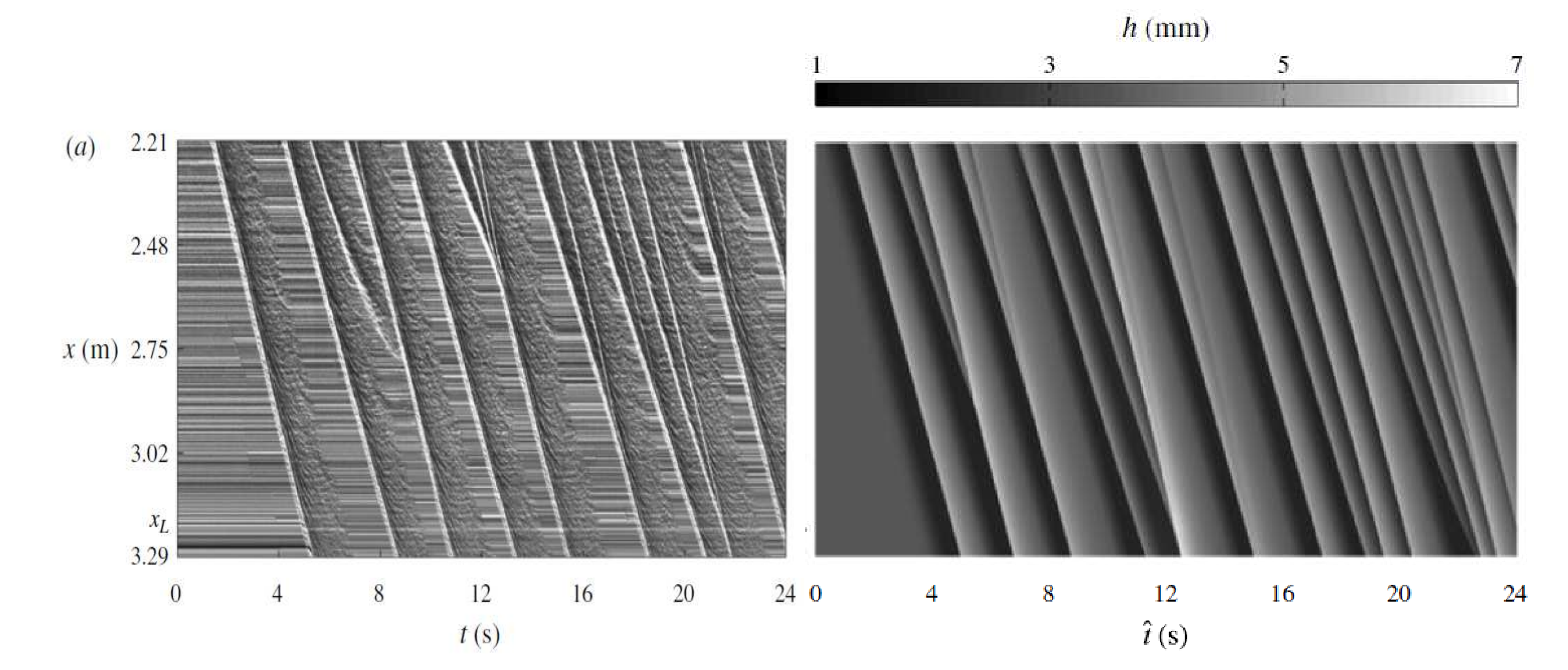

- Experimental space-time plot shows:-
  - regions of stationary material as horizontal straight lines
  - the wave-fronts as white lines
- very similar in computations (right)

Edwards & Gray (2015) *J. Fluid Mech.* **762**, 35-67.
Razis, Edwards, Gray & van der Weele (2014) *Phys. Fluids* **26**, 123305.

Theory has the potential to explain other situations ...

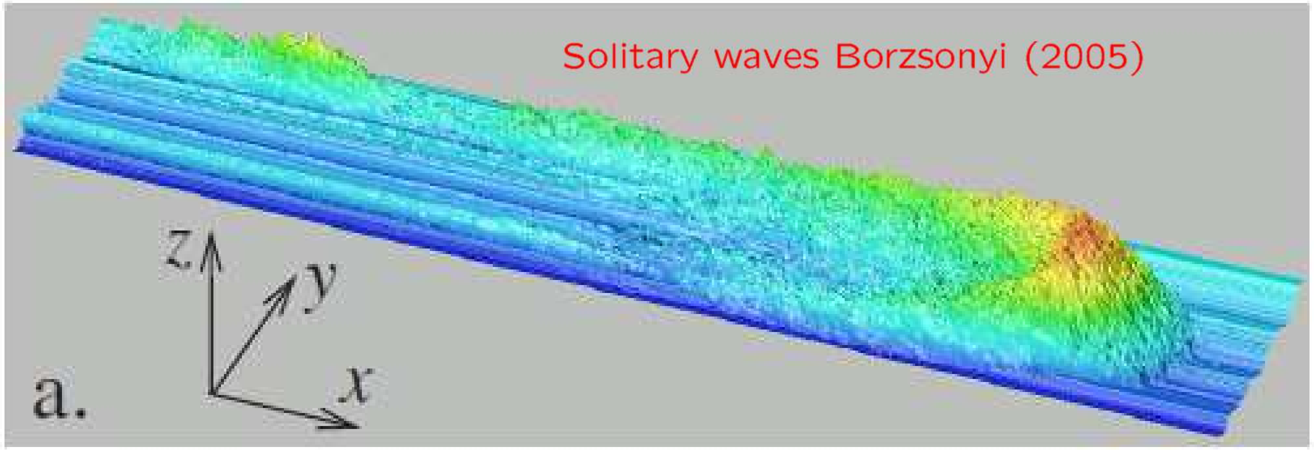

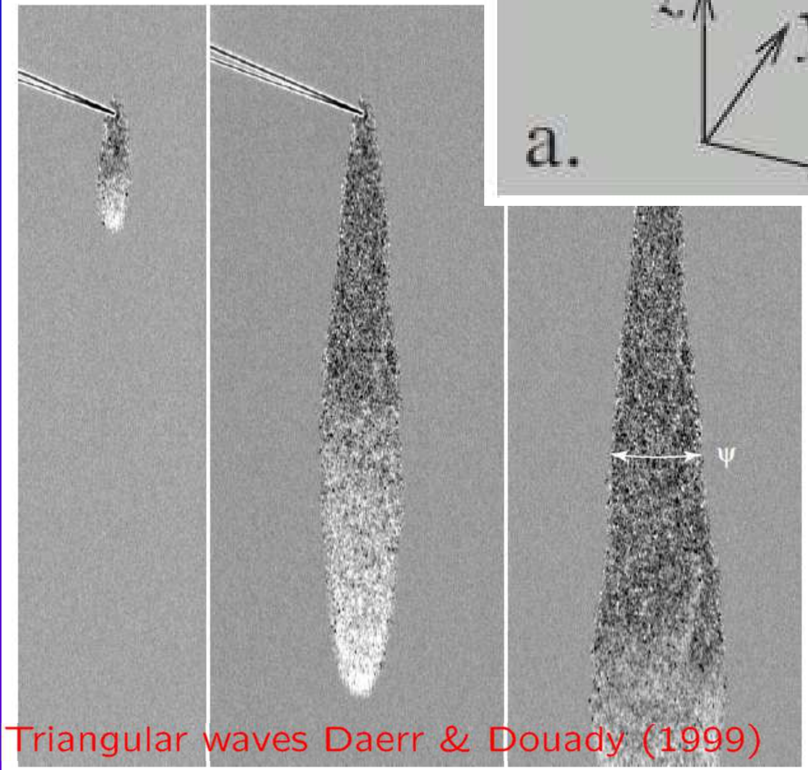

Figure 2 Evolution of a triangular avalanche ($\varphi = 30°$, $\delta\varphi = 1.5°$), showing the opening angle ψ. The time lapse between two images is 3.04 s. The pointed object is a pin used to trigger the avalanche, and indicates the origin of the avalanche.

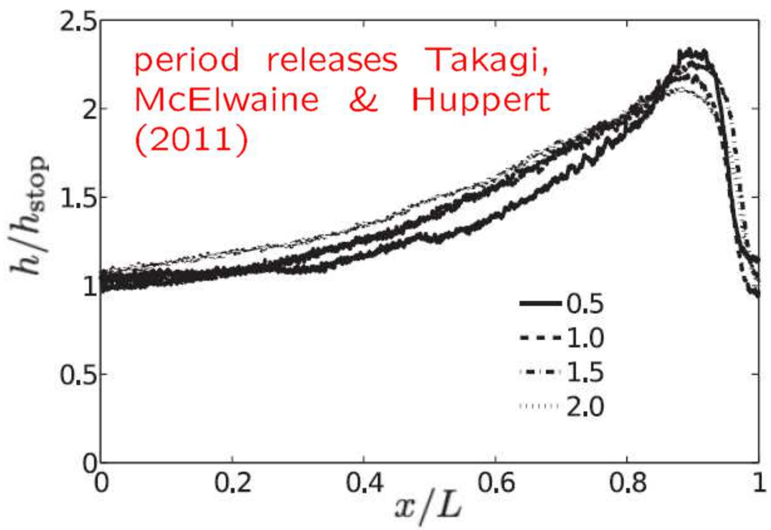

FIG. 22. Dimensional thickness profile of representative avalanches at 0.5, 1.0, 1.5, and 2.0 m down a 32° slope. The horizontal length is scaled by $L \approx 700$ mm, and the vertical length is scaled by $h_{stop} \approx 4.5$ mm. The mean profiles almost overlap, suggesting that

… and for segregation-induced fingering instabilities

Pouliquen, Delours & Savage (1997), Nature. **386**, 816-817.
Woodhouse *et al.* (2012), J. Fluid Mech. **709**, 543-580.

Kokelaar *et al* (2014) Earth Planet. Sci. Lett. 385, 172-180.

Schematic diagram for the levee formation process

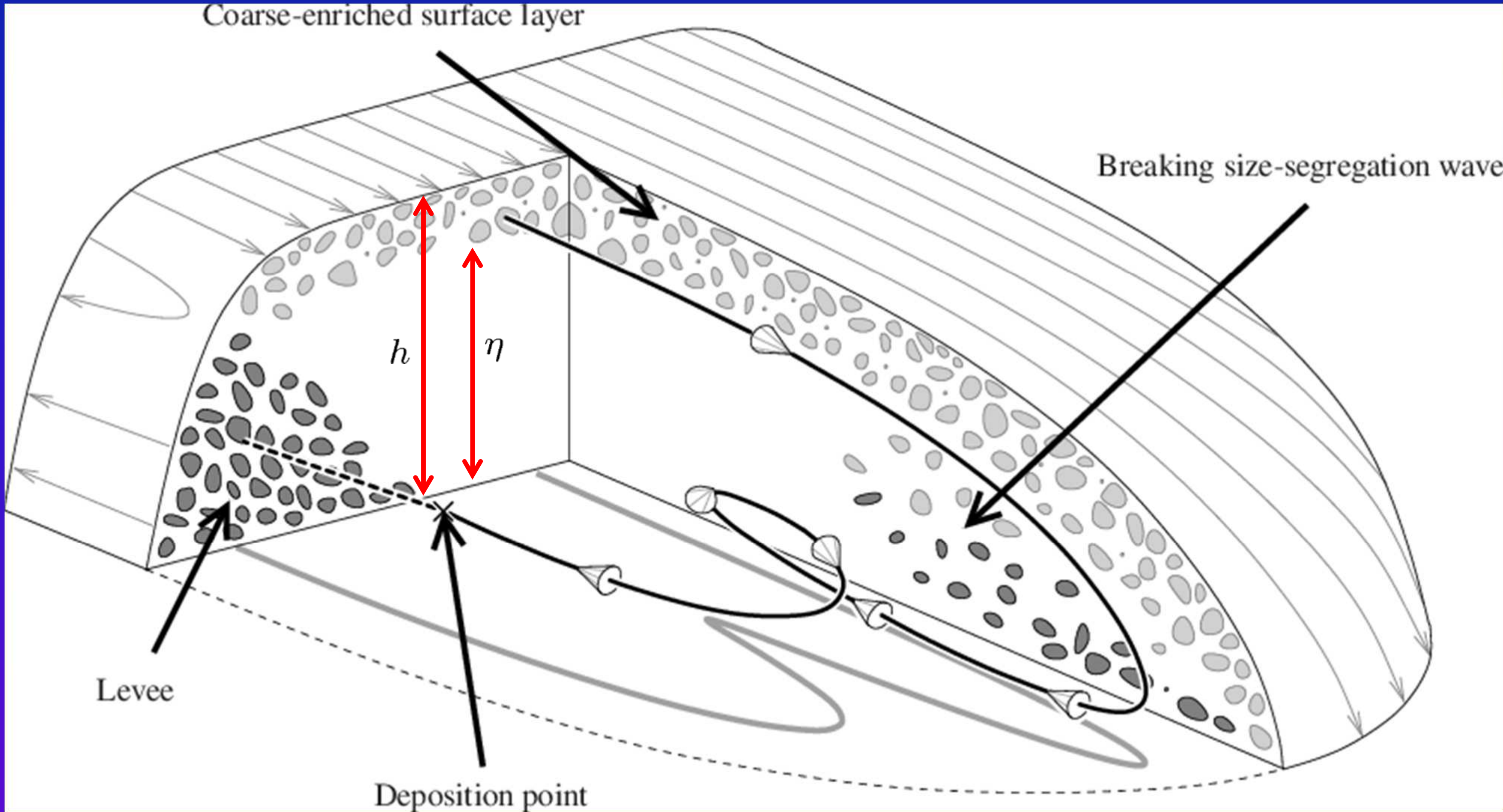

- larger particles are shouldered to the sides to create levees
- this is an example of a segregation-mobility feedback effect

USGS debris flow flume experiments summer 2009

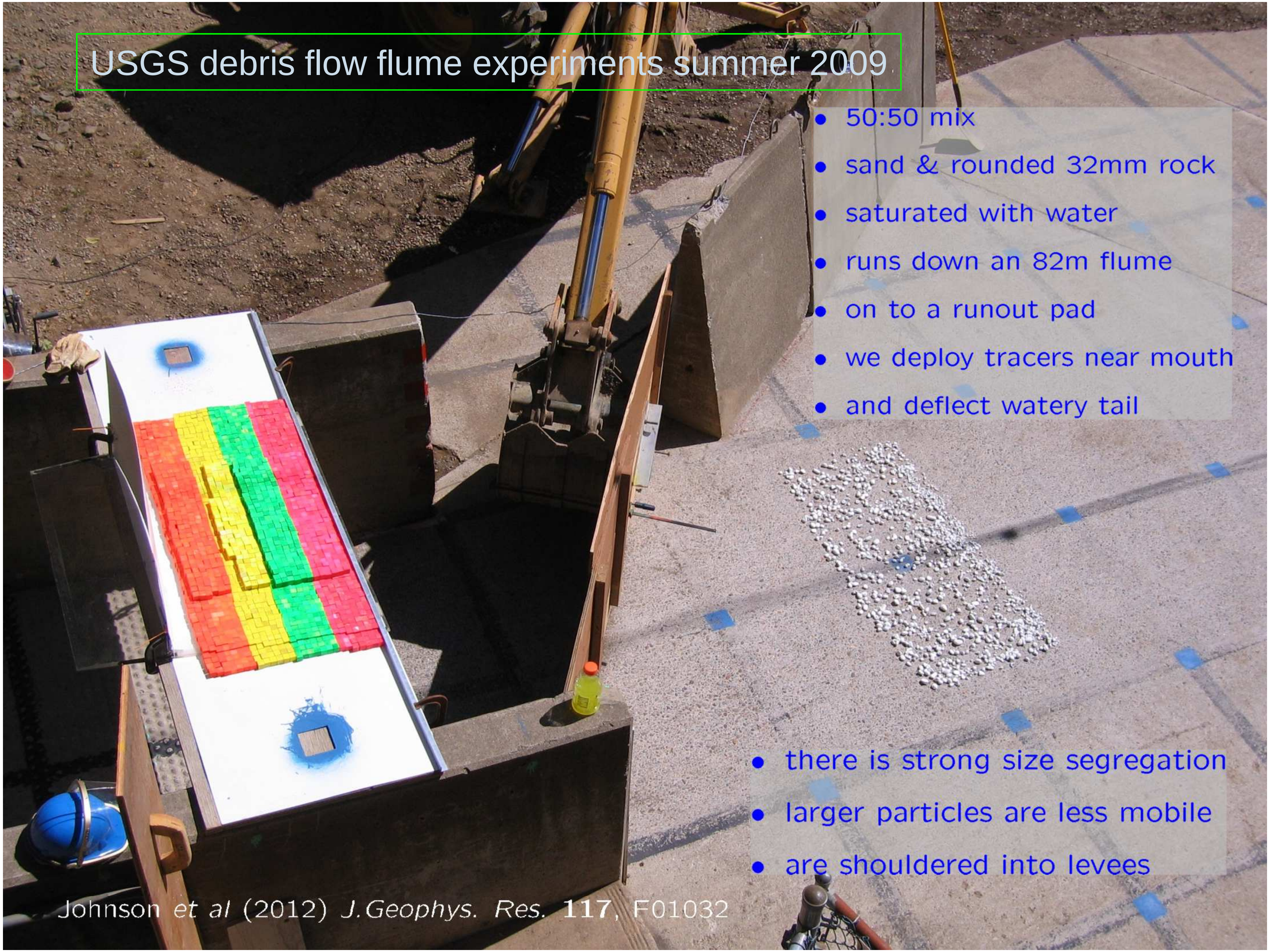

- 50:50 mix
- sand & rounded 32mm rock
- saturated with water
- runs down an 82m flume
- on to a runout pad
- we deploy tracers near mouth
- and deflect watery tail

- there is strong size segregation
- larger particles are less mobile
- are shouldered into levees

Johnson *et al* (2012) *J.Geophys. Res.* **117**, F01032


Measure velocity and levee emplacement time with 2cm cubes

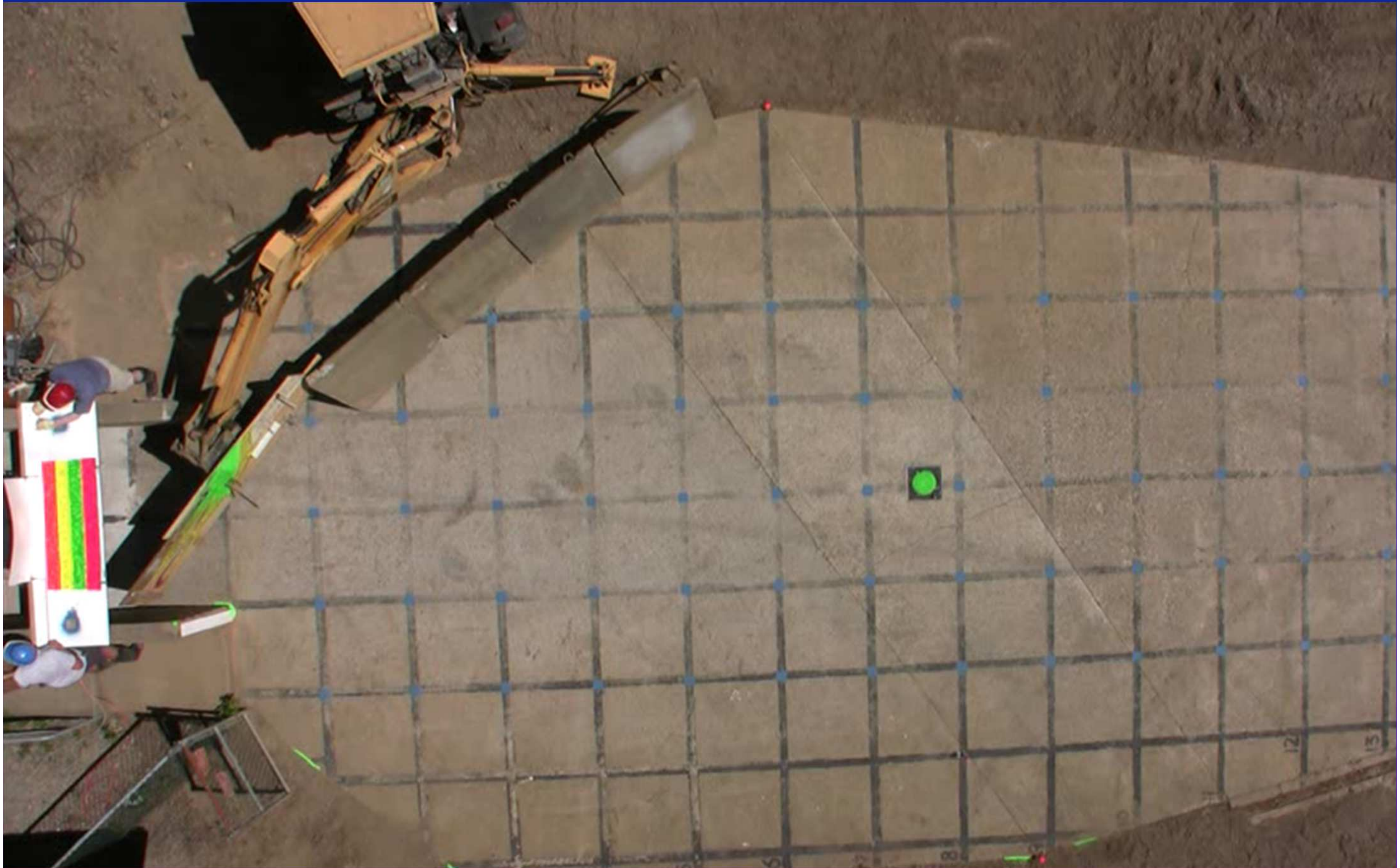

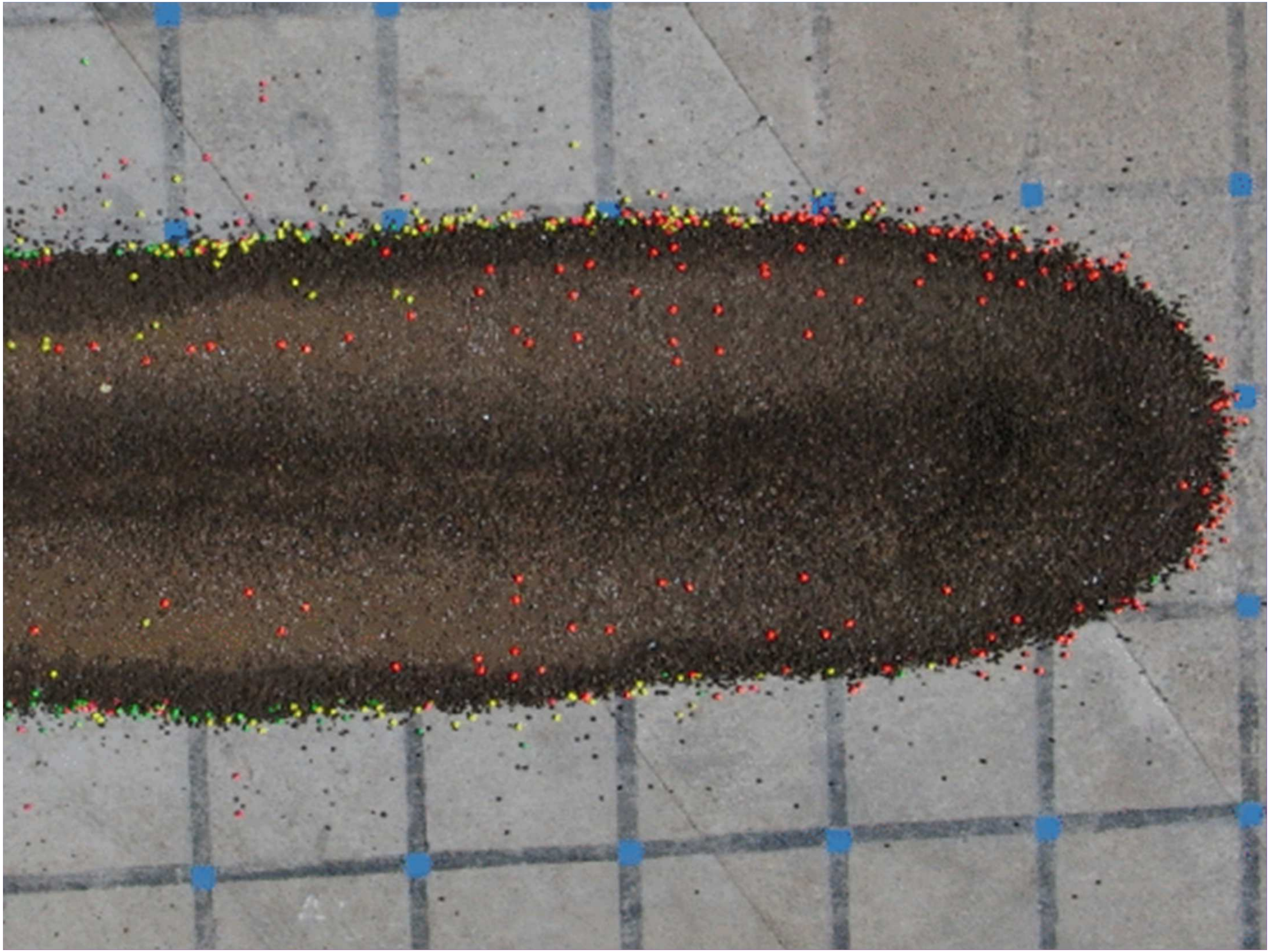

Surface velocity in stationary and front centred frames

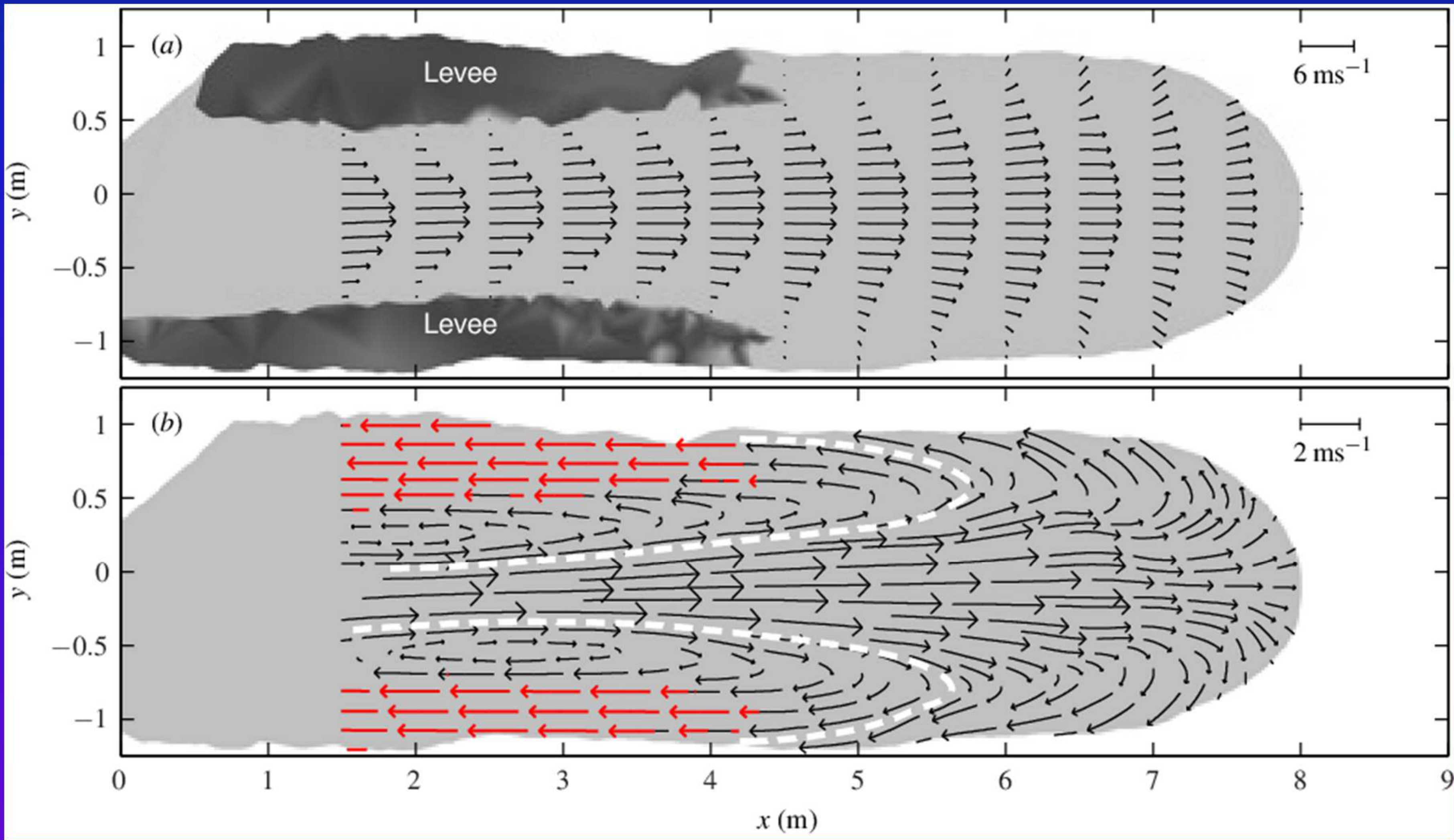

- $Oxyz$ are the downslope, cross-slope and normal directions

A simple kinematic model for 3D velocity field in the moving frame

- Bulk velocity $\mathbf{u} = (u, v, w)$ is assumed to be incompressible

$$\frac{\partial u}{\partial x} + \frac{\partial v}{\partial y} + \frac{\partial w}{\partial z} = 0$$

- Integrating through the avalanche depth h

$$\frac{\partial h}{\partial t} + \frac{\partial}{\partial x}(h\bar{u}) + \frac{\partial}{\partial y}(h\bar{v}) = 0$$

where the depth-averaged velocity

$$\bar{u} = \frac{1}{h}\int_0^h u\,dz, \qquad \bar{v} = \frac{1}{h}\int_0^h v\,dz$$

- In frame $\xi = x - u_F t$ the bulk flow is steady

$$\frac{\partial}{\partial \xi}\left(h\left(\bar{u} - u_F\right)\right) + \frac{\partial}{\partial y}(h\bar{v}) = 0$$

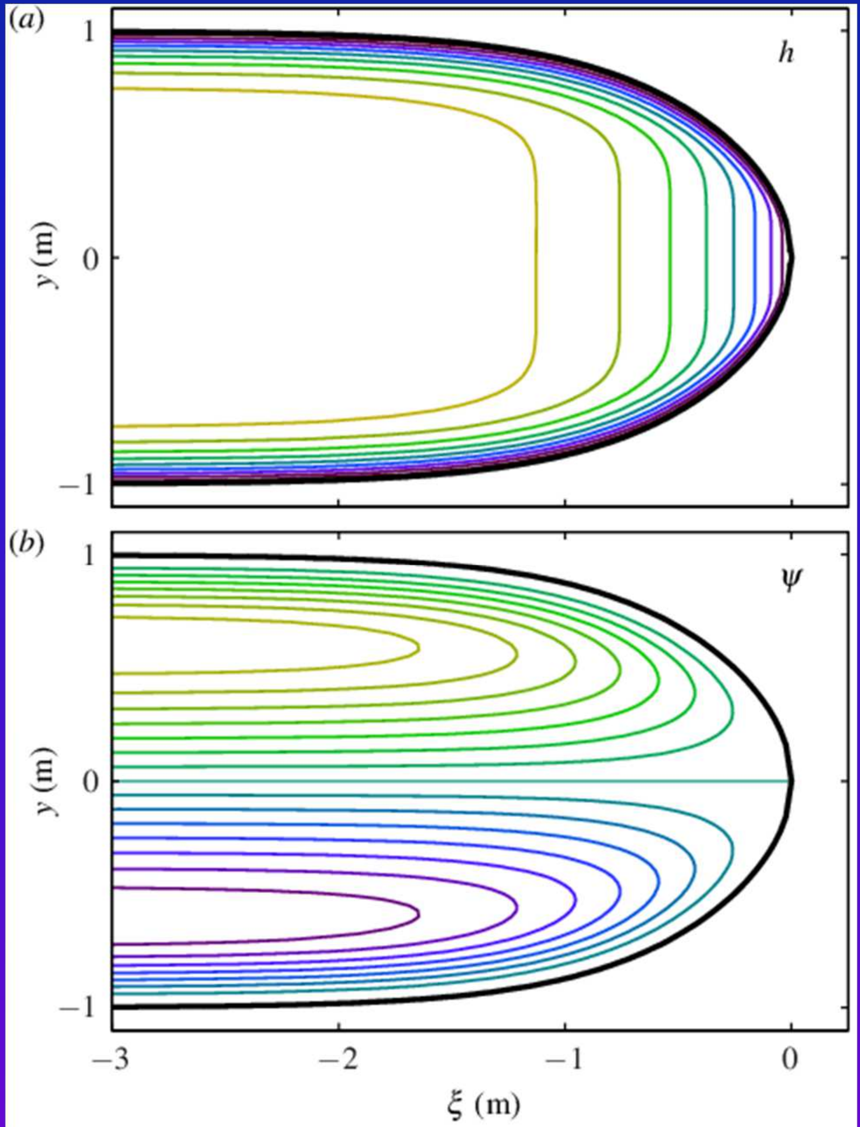

- define a streamfunction

$$\frac{\partial \psi}{\partial y} = h(\bar{u} - u_F), \qquad \frac{\partial \psi}{\partial \xi} = -h\bar{v}$$

- empirical front shape

$$y_0(\xi) = W\sqrt{\tanh\left(-\frac{\xi}{W}\right)}$$

- self similar thickness h

$$h(y_0, y) = \frac{H}{W}\left(\frac{y_0^{2n} - y^{2n}}{y_0^{2n-1}}\right)$$

- recirculating streamfunction

$$\psi(\xi, y) = \psi(y_0, y)$$

to approximate the flow

Reconstruction of the 3D velocity field

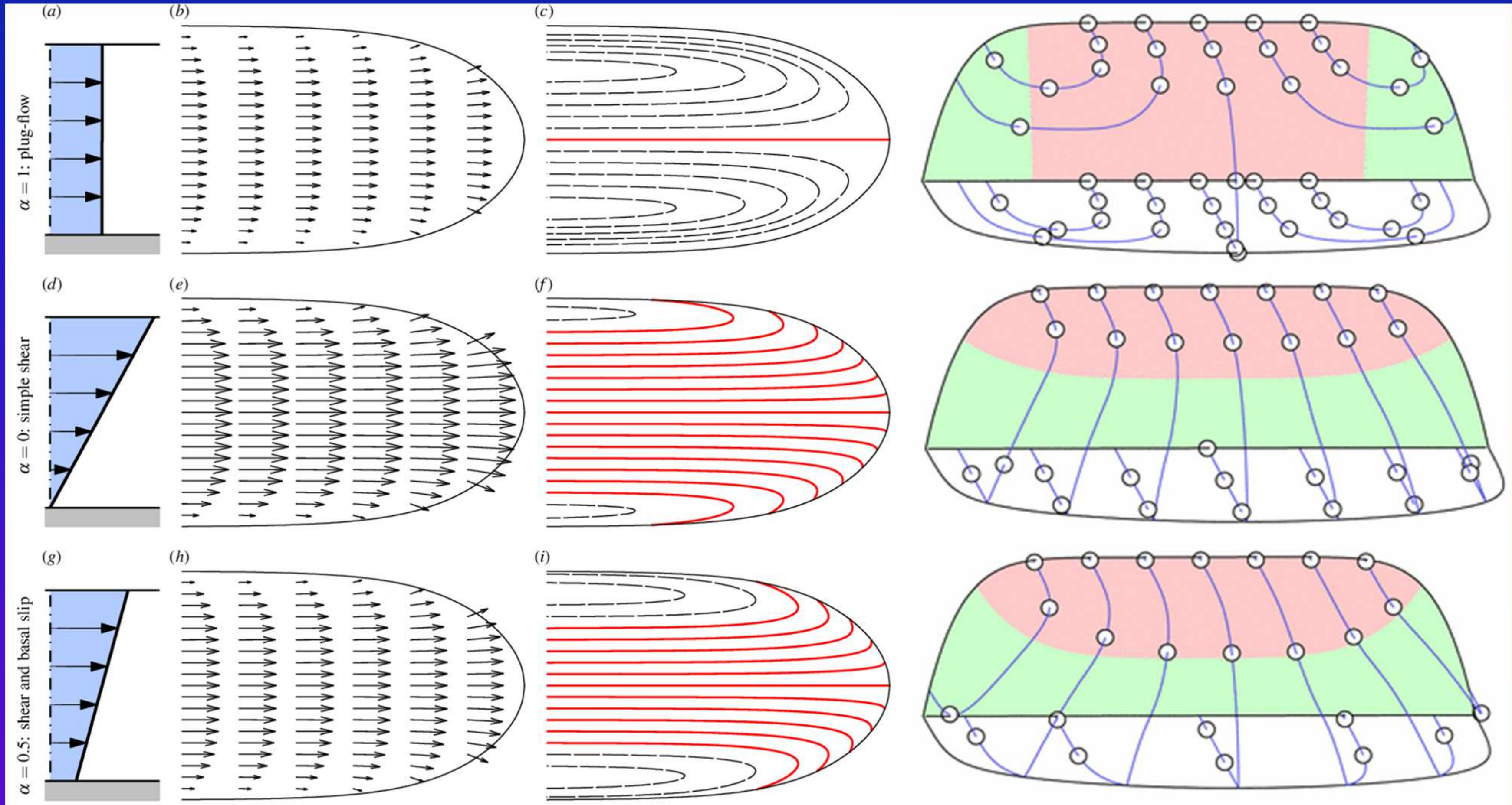

- assuming linear velocity profles with depth z

$$(u,v) = \left(\alpha + 2(1-\alpha)\frac{z}{h}\right)(\bar{u},\bar{v})$$


half cubes lie at the surface
mainly on top of the levee walls
in reverse order, i.e. orange, yellow, green, pink
Formation of coarse grained lateral levees and finer grained interior

Large particle tracer stone heights

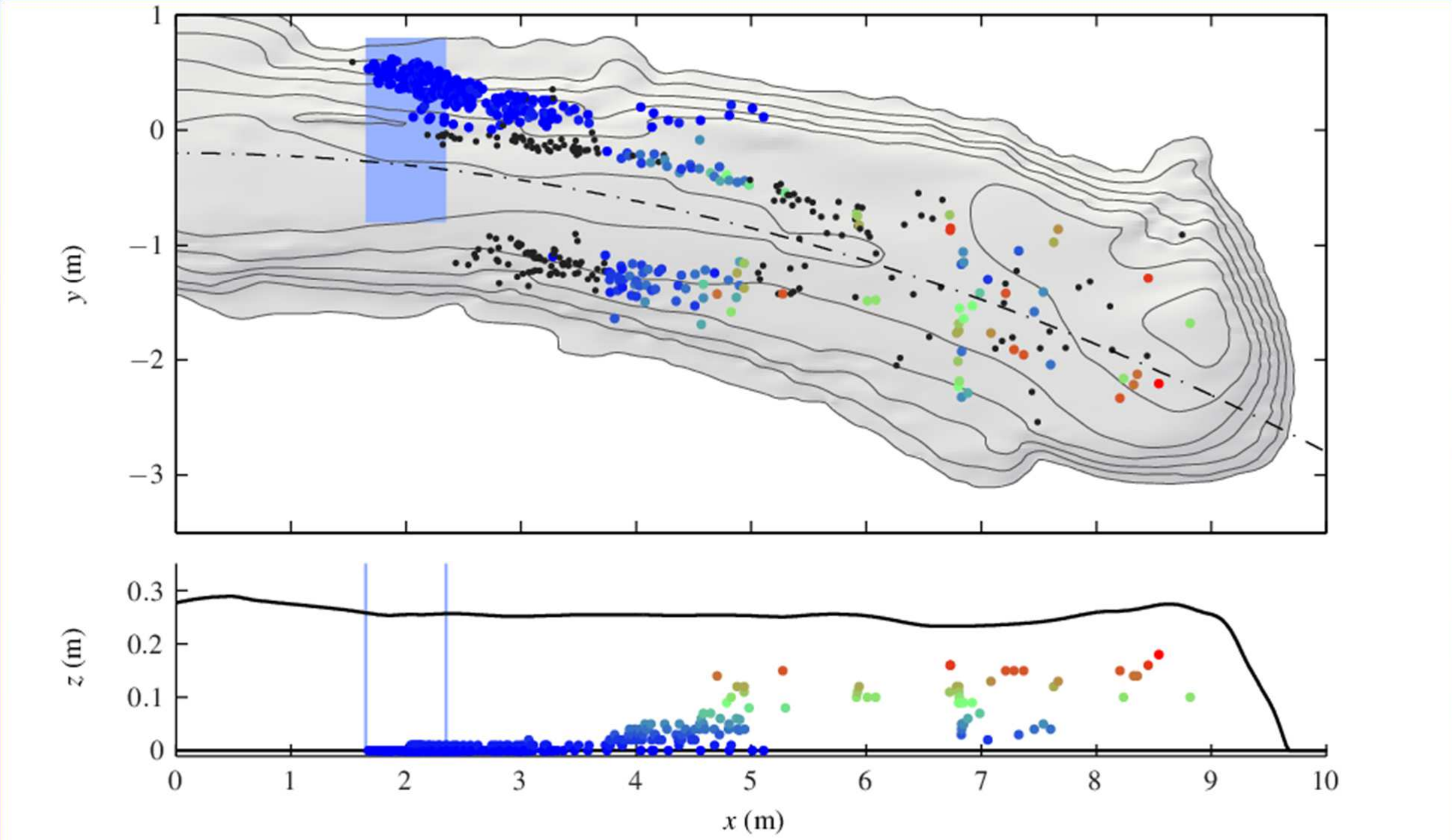

- Strong evidence for size segregation and recirculation
- BUT, stones never rise to the free surface again

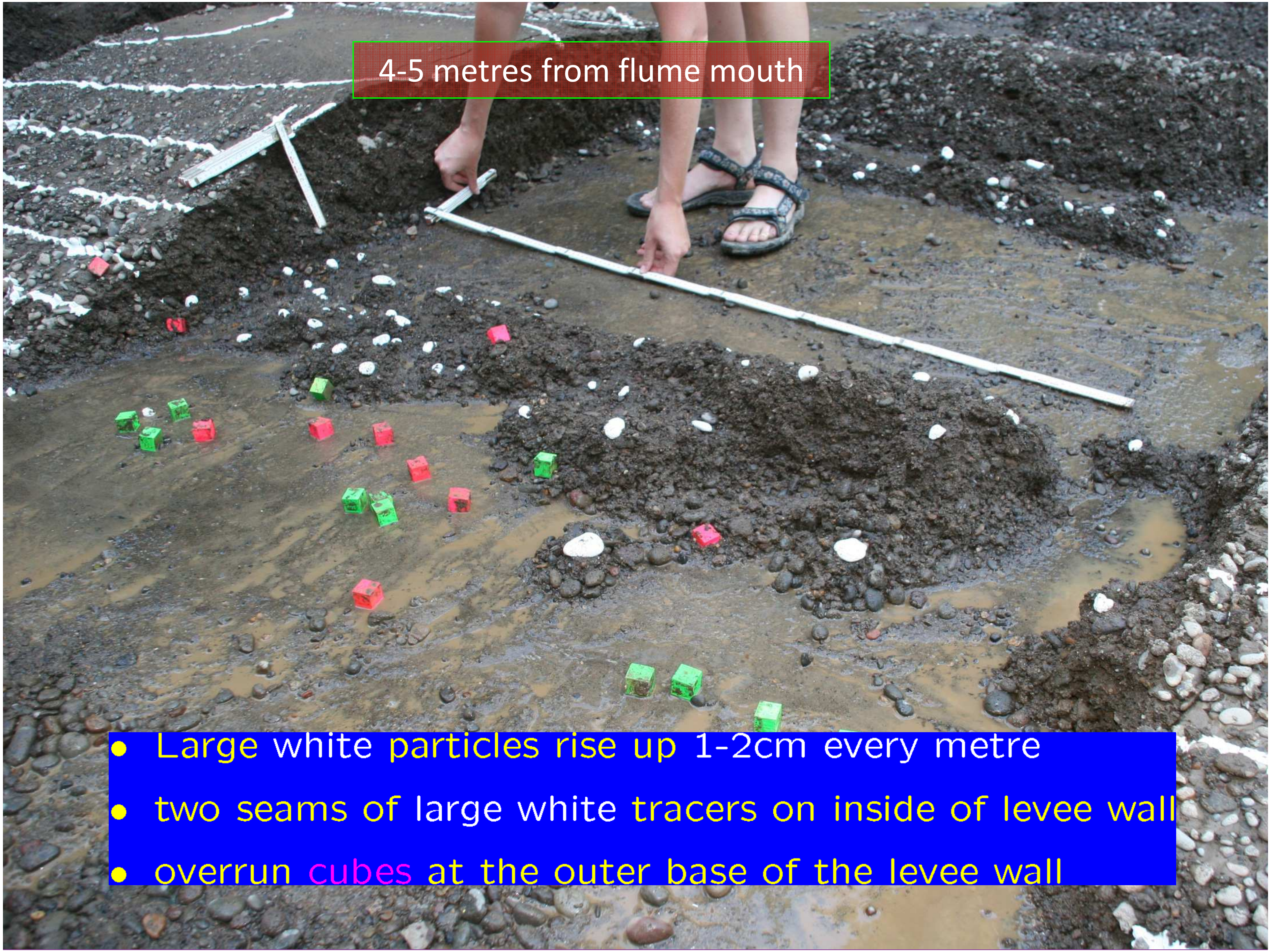
4-5 metres from flume mouth
• Large white particles rise up 1-2cm every metre
• two seams of large white tracers on inside of levee wall
• overrun cubes at the outer base of the levee wall


At the flow front
• central white grains carried to flow front and reach 15cm height
• orange cubes overrun at the front